

2018

METAL OXIDE CATALYSTS FOR THE DETECTION OF EXPLOSIVES: METHODOLOGY AND MECHANISM

Andrew S. Rossi
University of Rhode Island, rossia@my.uri.edu

Follow this and additional works at: <https://digitalcommons.uri.edu/theses>

Terms of Use

All rights reserved under copyright.

Recommended Citation

Rossi, Andrew S., "METAL OXIDE CATALYSTS FOR THE DETECTION OF EXPLOSIVES: METHODOLOGY AND MECHANISM" (2018). *Open Access Master's Theses*. Paper 1401.
<https://digitalcommons.uri.edu/theses/1401>

This Thesis is brought to you by the University of Rhode Island. It has been accepted for inclusion in Open Access Master's Theses by an authorized administrator of DigitalCommons@URI. For more information, please contact digitalcommons-group@uri.edu. For permission to reuse copyrighted content, contact the author directly.

METAL OXIDE CATALYSTS FOR THE DETECTION OF
EXPLOSIVES: METHODOLOGY AND MECHANISM

BY

ANDREW S. ROSSI

A THESIS SUBMITTED IN PARTIAL FULFILLMENT OF THE
REQUIREMENTS FOR THE DEGREE OF
MASTER OF SCIENCE
IN
CHEMICAL ENGINEERING

UNIVERSITY OF RHODE ISLAND

2018

MASTER OF SCIENCE IN CHEMICAL ENGINEERING THESIS
OF
ANDREW S. ROSSI

APPROVED:

Thesis Committee:

Major Professor Otto Gregory

Tao Wei

Everett Crisman

Nasser H. Zawia
DEAN OF THE GRADUATE SCHOOL

UNIVERSITY OF RHODE ISLAND
2018

ABSTRACT

At the University of Rhode Island's Sensors and Surface Technology Partnership, a sensor platform has been fabricated that is capable of detecting explosive vapor at the ppb level. This sensor utilizes differential signal processing between a catalyzed microheater and a bare reference microheater to detect heat effects from catalyst-analyte interactions. The reaction mechanism behind these catalytic heat effects is highly debated and was originally thought to be due to chemisorption and catalytic decomposition of explosive vapor molecules [1]. The true mechanism of detection has been proven to be oxidation or reduction of the metal oxide catalyst to higher or lower oxidation states.

This mechanism was revealed thanks to the increased sensitivity of the thermodynamic sensor created by the significant decrease in thermal mass to the nickel microheater platform. This increased sensitivity allowed for the detection of heat effects at significantly lower temperatures thus new trends in sensor behavior were observed as sensors using different metal oxide catalysts were swept from room temperature to 500°C. Activation energy calculations for SnO₂ reduction, Cu₂O oxidation, and ZnO reduction were consistent with activation energy values presented by literature. Further evidence that these metal oxide catalysts are changing oxidation state was presented through SEM imaging of a tin oxide catalyst.

Sensor selectivity was also investigated relating to the differentiation between different explosive compounds such as TATP or 2,4-DNT. Reference sensors not employing a metal oxide catalyst are not responsive to TATP however a small heat effect is observed when the sensor is subjected to 2,4-DNT vapor. In order to identify

specific explosive compounds, “fingerprint” plots were created using multiple different catalysts exposed to the same analyte. Plots were created for TATP, DADP, and 2,4-DNT and each plot has unique features. These features allow for the differentiation between individual explosive compounds.

ACKNOWLEDGMENTS

I would like to thank all of the undergraduate students who helped me throughout my two years as a graduate research assistant including Spencer Fusco, Jonathan Cummings, Alyssa Kelly, and especially Peter Ricci for his tremendous dedication and unwavering belief in how far we can take this project. Their help with testing procedures, lithography, and brainstorming sessions really accelerated the project and helped take it to where it is today.

I would also like to thank Matt Ricci, Kevin Rivera, Tommy Muth, and Mike Platek for their patience and knowledge while teaching me to use equipment in the laboratory such as the sputtering machines, furnaces, and lithographic technology. Mike Platek was especially helpful for the time he spent with our group collecting SEM images and performing XPS for our group.

I would like to greatly thank Dr. Otto Gregory for being such a great teacher and mentor throughout not just my graduate career, but my entire time at URI. I am incredibly thankful for the opportunity he gave me as an undergraduate to work in his laboratory. His laboratory helped me to realize that my passion for chemical engineering is centered on my interest in materials science.

I would like to thank my family, especially my parents, Tom and Joan Rossi, for their constant support throughout my entire education, both financially and emotionally. Because of the constant encouragement and kindness they showed me, I was set up with the tools I needed to complete my engineering education and to be a better person all together.

Lastly, I would like to thank my girlfriend, Justyna Falat, for her ability to talk me through all of the stressful situations I've encountered. I greatly appreciate all of her help over the past few years and also for carrying me through organic chemistry.

TABLE OF CONTENTS

ABSTRACT.....	ii
ACKNOWLEDGMENTS	iv
TABLE OF CONTENTS.....	vi
LIST OF FIGURES	vii
CHAPTER 1: INTRODUCTION	1
CHAPTER 2: LITERATURE REVIEW	3
2.1: Energetic Material And Explosive Classification.....	3
2.2: Triacetone Triperoxide (TATP) Properties.....	4
2.3: TATP Terror Attacks	6
2.4: Other Explosive Detection Techniques.....	7
2.5: The Need For A Portable Electronic Dog Nose	13
2.6: Metal Oxidation And Reduction Reactions	14
2.7: Previous Uri Explosive Vapor Sensor Work	15
CHAPTER 3: METHODOLOGY	21
3.1: Sensor Fabrication And Heating.....	21
3.2: Lab Testing Setup And Protocol.....	23
3.3: “Portable” Elctronic Detection System	221
CHAPTER 4: DATA AND RESULTS	28
4.1: Portable System Testing	28
4.1.1: Humid Environment Testing.....	28
4.1.2: Nitrogen Annealing.....	29
4.1.3: Flow Rate Optimization.....	30

4.2: Detection Mechanism	32
4.2.1: Oxidation and Reduction of Tin Oxide Catalysts	32
4.2.2: Oxidation and Reduction of Copper Oxide Catalysts	35
4.2.3: Reduction of Zinc Oxide Catalysts	37
4.2.4: SEM Confirmation	39
4.3: Improved Selectivity via Catalyst Selection	41
CHAPTER 5: CONCLUSION	46
5.1: Main Conclusions	46
5.2: Future Work	48
BIBLIOGRAPHY	51

LIST OF FIGURES

FIGURE	PAGE
Figure 1. 2D structure of triacetone triperoxide.....	5
Figure 2. Schematic of an IMS detection system. A vapor sample enters the IMS system, becomes ionized, and those ions are subjected to an electric field. Ions drift based on their mass to charge ratio and these drift times are collected by a data acquisition system	8
Figure 3. (top) photograph of what seems to be typical luggage. (bottom) CT image of the same luggage as above. The doll in the top image is an IED containing explosive that is highlighted in red by the CT image below	12
Figure 4. Preconcentration test conducted using a stoichiometric SnO ₂ catalyst and 2,6-DNT using the dynamic control method: (1) beginning of DNT delivery to sensors (2) preconcentrator begins thermal desorption (3) preconcentrator is turned off and reference gas is reintroduced to the chambers	16
Figure 5. Orthogonal response of a tin oxide catalyst to 2,6-DNT vapor. Thermodynamic signal is shown in blue while the conductometric signal is shown in red.....	17
Figure 6. Tin oxide sensor responses to varying TATP concentration. Sensors are operating at 500°C. The orange response curve is from a sensor using a flat, as sputtered catalyst and the blue curves employ a sensor with nanowire catalyst supports to increase catalytic surface area.....	18

Figure 7. The difference in sensor platform sensitivity is highlighted here by the difference in responses from the substrate using microheater on an alumina substrate (blue curve) and the free standing low mass nickel microheater (orange curve). Both sensors used the same tin oxide catalyst, were exposed to the same concentration of TATP (20ppm), and were held at the same operating temperature (500°C)..... 19

Figure 8. Nickel coil used as a microheater in the sensor platform. 22

Figure 9. Schematic of the testing apparatus used in the testing procedures described. 24

Figure 10. Schematic of the portable ETD system. A power supply is still needed to complete the ETD system however in order to test the apparatus, a power strip connected to an external power source has replaced the power source shown in the schematic..... 26

Figure 11. SnO₂ catalyzed thermodynamic sensor response to TATP under various conditions of humidity. Installing an empty vessel downstream from the TATP introduced a dilution effect (red curve), which lowered the response significantly compared to the portable ETD system operating using no flask. 29

Figure 12. Effect of nitrogen annealing on a SnO₂ sensor when exposed to 2.8ppm TATP. Red curve represents sensor response after hours of testing in relatively high humidity conditions..... 30

Figure 13. Sensor responses to 20ppm TATP utilizing a SnO sensor operating at 500°C. Flow rates of 25, 130, 170, and 210 sccm were investigated. 31

Figure 14. Sensor response of a SnO catalyst to TATP in air at varying temperatures. The inset figure highlights the first 30 seconds of the experiment where the sensor temperature of 375°C initially responded exothermically, before a much larger endothermic heat effect was observed 33

Figure 15. Sensor response of a SnO ₂ catalyst to TATP in air at various temperatures	34
Figure 16. Sensor response of a Cu ₂ O catalyst to TATP in air at various temperatures	36
Figure 17. Sensor response of a CuO catalyst to TATP in air at various temperatures.	37
Figure 18. Sensor response of ZnO catalyst (before and after heat treatment) to TATP in air at varying temperatures.....	38
Figure 19. SEM fractograph of a nickel microheater coated with a SnO catalyst after exposure to TATP vapor.	40
Figure 20. Catalyzed (blue) and reference (orange) sensor response to 2,4-DNT vapors. Both sensors are heated to 375°C and exhibit significant endothermic signals.	42
Figure 21. Catalyzed (blue) and reference (orange) sensor response to TATP vapor. Both sensors are heated to 375°C and only the catalyzed sensor exhibits a significant endothermic signal	43
Figure 22. SnO ₂ , ZnO, CuO, and FeO sensor responses to TATP vapor at sensor temperatures of 500°C	44
Figure 23. SnO ₂ , ZnO, CuO, and FeO sensor responses to DADP vapor at sensor temperatures of 500°C	45
Figure 24. SnO ₂ , ZnO, CuO, and FeO sensor responses to 2,4-DNT vapor at sensor temperatures of 500°	45
Figure 25. Modified sensor housing capable of holding up to 9 sensor devices at once.	49

CHAPTER 1

INTRODUCTION

All too commonly, terror groups utilize improvised explosive devices (IEDs) to cause harm to innocent civilians. These IEDs often times incorporate an explosive, triacetone triperoxide (TATP), as the detonator or main charge. This compound is incredibly popular amongst terrorist groups because of its ease of fabrication and availability of its precursors. While extremely dangerous, it is possible to produce TATP by utilizing readily available precursors including acetone and hydrogen peroxide that can be purchased at a local pharmacy without attracting attention.

There have been a number of recent incidents where TATP has been used as an initiator and caused serious injury to civilians. These include the 2016 Brussels airport bombing, the 2017 Manchester concert bombing, and most recently the 2018 Surabaya church bombings. Incidents such as these have resulted in hundreds of deaths, thousands of injuries, and millions of dollars' worth of destruction. While many populated venues have security checkpoints, the protocols employed are not one hundred percent effective. Current state of the art schemes for explosives detection rely on trained dogs to sniff out potential threats. These dogs can be very expensive to train and maintain, require a handler at all times, and are easily fatigued and distracted. The creation of a low cost, continuous electronic trace detection system (ETD) may eliminate the need for these bomb sniffing dogs and thus improve the efficiency of security checkpoints to detect for explosives.

A sensor capable of detecting TATP in the vapor phase in real time in an attempt to protect the public from explosive threats [1-3], has been under development at The University of Rhode Island for some time. This sensor has shown the capability to detect TATP on the ppb level; however the exact mechanism responsible for such low detection levels has been highly debated, and the superb selectivity to compounds like TATP has been the focus of several investigations. The following work shows that the sensing mechanism relies on the oxidation or reduction of the metal oxide catalyst employed for decomposition, and the subsequent heat effects that accompany these reactions. Through this newfound sensing mechanism, the possibility of improving sensor selectivity to explosives is also described within.

Over the past few years, improvements have been made to the sensor such that the detection of TATP vapor is possible at the single ppb level (verified at the Naval Research Laboratory's Vapor Test Bed). These improvements included the use of an extremely low mass microheater as opposed to a flat ceramic substrate utilizing a sputtered thin film microheater [1]. This improvement has made detection possible at significantly lower temperatures and thus, the response was observed at lower temperatures. This shift in response gave further insight into the mechanism behind explosive vapor detection.

CHAPTER 2

LITERATURE REVIEW

Chapter 2.1: Energetic material and explosive classifications

Explosives and energetic material can be classified into different subgroups depending on the explosive's performance [4]. The first branch of explosives differentiates between low explosives and high explosives. Low explosives, when initiated, typically burn slowly or deflagrate. These explosives are used in pyrotechnics (ex: fireworks) or propellants (ex: rocket fuel). The second branch of explosives is known as high explosives, which generally release much more energy and consequently perform superior to low explosives. High explosives release significantly more energy upon decomposition.

Contrary to popular belief, damage from a high explosive does not occur from the heat of the reaction but instead the speed of expansion from solid or liquid explosive forming a gas upon initiation/decomposition [4]. Nitro or peroxide groups in explosive compounds commonly decompose in these violent reactions to form gaseous, low density compounds such as N_2 or O_2 . This expansion creates a wall of pressure, known as a shockwave, which propagates through the explosive and out into the surrounding area. An explosion is technically classified or defined as “a violent expansion in which energy is transmitted outward as a shock wave” [5]. Frequently, improvised explosive devices (IEDs) will incorporate shrapnel into the device to be thrown by this pressure wave to cause more harm to surrounding people.

High explosives themselves are subdivided into groups known as primary explosives and secondary explosives [4,6]. The difference in these two groups is largely due to the explosive's density. Low density explosives are much easier to initiate yet have a much slower reaction speed, while high density explosives are hard to initiate but perform at higher velocities than lower density explosives. Often times, low density explosives are used to initiate a high density explosive in what is known as an explosive chain. Within the primary explosives category there are even more subcategories depending on an explosives primary usage (military or industrial explosives), or chemical composition (nitrogen based or peroxide based).

Typically, most explosives are nitrogen based, such as trinitrotoluene (TNT), pentaerythritol tetranitrate (PETN), and nitroglycerin (NG). These explosives rely on NO_2 functional groups for their explosive properties. Peroxide based explosives such as TATP do not contain this NO_2 group and thus detection techniques that rely on the identification of this functional group in the explosive are not reliable.

Chapter 2.2: Triacetone Triperoxide (TATP) Properties

The sensitivity and lack of a nitro group in TATP result in properties that make TATP uniquely difficult to detect. TATP has limited fluorescent properties [7] and decomposes when exposed to moderately high temperatures (100°C). TATP is a moderate performing explosive, and because of its tendency to easily initiate upon the introduction of stimuli such as high temperature, friction, or shock, it is generally not used by military organizations [6].

One of the few properties of TATP that makes the explosive more attractive for detection than other energetic compounds is the extremely high vapor pressure exhibited by TATP. The vapor pressure of TATP at room temperature is 4.65×10^{-2} Torr which is order of magnitude higher than other commonly used explosives such as PETN (1.16×10^{-8} Torr) and TNT (5.50×10^{-6} Torr) [8]. Due to this high vapor pressure, TATP molecules are relatively highly concentrated in the vapor phase surrounding the solid explosive. Therefore, our group has concluded that the best chance to quickly and effectively alert the public to TATP explosive threats is by interrogating vapor surrounding people or containers that may be concealing IEDs utilizing TATP.

TATP is a relatively large molecule with a molar mass of 222g/mol and is comprised of carbon, oxygen, and hydrogen atoms (molecular formula: $C_9H_{18}O_6$). The elemental structure of TATP is shown below in figure 1 [9].

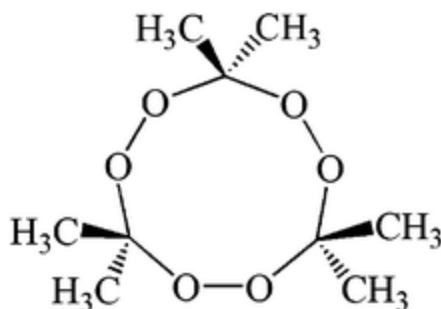


Figure 1: 2D structure of triacetone triperoxide [9].

Oxley et al. [10] reports the main decomposition products of TATP are acetone and carbon dioxide however it has been argued by Hiyoshi et al. [11] that methane and carbon dioxide are the main decomposition products of TATP upon high heating rates. These different decomposition products play a significant role in the detection mechanism presented within.

Chapter 2.3: TATP Terror Attacks

In contrast to other explosive compounds, TATP can be fabricated using precursors that are readily available at most pharmacies or department stores, such as sulfuric acid hydrogen peroxide, and acetone. Certain hair products contain significant quantities of hydrogen peroxide and acetone can be found in products such as nail polish remover. Sadly, due to the internet [6] and the ease of distribution of information made possible by the internet, it is all too easy to learn techniques that teach how to fabricate crystalline TATP. This information combined with the ability of the public to buy explosive precursors, makes TATP a popular explosive used amongst terror organizations.

One of the most devastating terror attacks utilizing TATP explosives was the “7/7” attacks in London [12]. On July 7th, 2005 multiple suicide bombers using explosives including TATP detonated explosives in 3 underground trains as well as a bus in London, France. In total 52 people lost their lives and more than 770 others were injured.

Attacks have been made on other public venues such as churches, concert halls, and airports. In 2016 a Brussels airport, known as Zaventem, was attacked by multiple suicide bombers carrying IEDs that incorporated TATP and shrapnel [13]. The first terrorist caused an explosion that initiated mass panic, and as civilians ran towards the exit of the airport, a second bomber was waiting with a separate device. In this incident 16 people died and hundreds more were injured.

In 2017, at a concert hall in Manchester, a single suicide bomber was able to successfully detonate another IED utilizing TATP and shrapnel, which killed 22 innocent civilians [14]. This man was able to create TATP with precursors that he bought at stores in the surrounding area, just a few days before the incident. Most recently, three churches in Surabaya, Indonesia were attacked by suicide bombers in May of 2018[15]. Over 13 people were killed and many more were significantly injured. It is extremely evident based on the frequency of attacks that TATP is a very popular explosive used in terror attacks due to the availability of its precursors and difficulty to detect.

Chapter 2.4: Other Explosive Detection Techniques

Currently, the main method of detection used in airports by the Transportation Security Administration (TSA) incorporates the use of computerized tomography (CT) tunnels. These tunnels combine multiple X-ray measurements taken at different angles to generate an image of a luggage's contents [16, 17]. This image is then examined by a TSA officer trained to identify contraband such as weapons, drugs, or IEDs. The main flaw with this detection technique comes from user error. A single TSA agent screens over 600 bags in one hour [17] and thus it is extremely easy for contraband to go unnoticed.

Recently (November 2017) the Department of Homeland Security (DHS) conducted an undercover operation to test the effectiveness of TSA screening techniques [18]. This operation disguised DHS officials as civilians carrying contraband and sent them through several security checkpoints at different airports.

Although the exact details of operation are confidential, a DHS official commented that TSA failure rate was “in the ballpark” of 80 percent [18]. Although the contraband used in this investigation may not have been exclusively IED threats, this investigation highlights that there are major flaws in the methods used by TSA agents to screen for contraband.

This extremely high failure rate exhibited by TSA officials can be mitigated with the incorporation of technology that screens for contraband and while eliminating the possibility for operator error, hence the need for an explosive sensor capable of detecting explosive contraband. Many of these platforms do exist that are capable of detecting either solid explosive or explosive vapor at very low concentrations, however each of these platforms has their own drawbacks in terms of continuously detecting for explosives quickly and effectively in public settings.

Ion mobility spectrometry (IMS) is a widely used technique for identifying explosives in the vapor phase. This technique relies on the drift characteristics of vapor molecules after they have been ionized [16]. These ions are then subjected to an electric field and consequently drift for a specific period of time depending on their mass to charge ratio (figure 2).

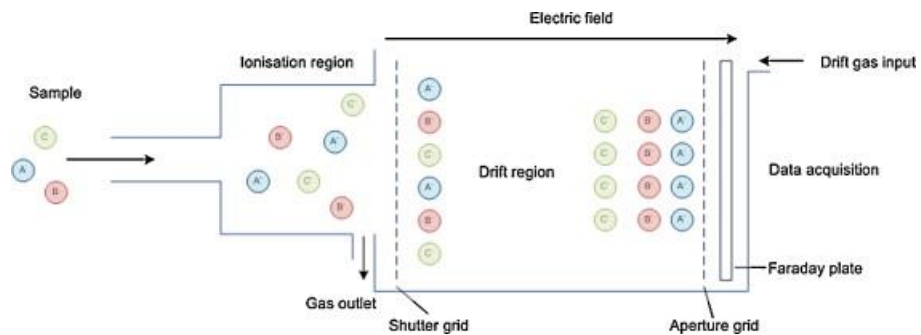


Figure 2: Schematic of an IMS detection system. A vapor sample enters the IMS system, becomes ionized, and those ions are subjected to an electric field. Ions drift based on their mass to charge ratio and these drift times are collected by a data acquisition system [16].

Based on these drift times, the mass to charge ratio of the molecules in the vapor phase can be derived and compared to previously cataloged data to identify the molecules present in the vapor [16]. IMS techniques have been proposed for the detection of TATP [19] however this method has its own drawbacks. While IMS is an extremely fast detection method (about 3 seconds to positively identify TATP) it also has a very poor detection limit (above 100s of ppm).

Mullen et al. used IMS in the form of single photon laser ionization techniques in conjunction with time of flight mass spectrometry (TOF/MS) to be able to detect not just TATP but other nitrogen based explosives at the ppb level in the vapor phase [20]. However, this technique requires high power requirements and many pieces of expensive equipment that would not be economically feasible for public venues, such as concerts halls and airports, to implement in their security lines [16, 20].

Another detection method, fluorescence, involves the excitation of molecules through a chemical reaction to induce the release of light which can then be used to identify individual molecules [16]. Fluorescent identification and gas chromatography techniques have been investigated in an attempt to identify TATP vapors specifically, however TATP itself does not exhibit significant fluorescence characteristics [7] and GC is difficult to perform due to the thermolability (tendency to decompose under moderate heat) of TATP [19]. Interestingly, TATP can be indirectly detected by using sulfuric acid as a catalyst to decompose TATP molecules to hydrogen peroxide (H_2O_2), which is more fluorescently active. It is also possible to detect TATP through GC in combination with mass spectrometry if the temperature of the GC column is

held in a low temperature range [21], however because of the temperature dependence on separation time, this process is too time consuming to be implemented in fast moving security lines.

Other separation and ionization techniques such as liquid chromatography [22] as well as dielectric barrier discharge ionization-mass spectrometry (DBDI-MS) [23] have successfully been used to identify TATP in extremely small quantities. Sadly, because these techniques detect either solid or solutionized TATP and they are ineffective at detecting explosive unless individuals were independently swabbed for residue, which is incredibly time consuming.

Colorimetric sensors for the detection of explosive vapor show exemplary qualities in terms of selectivity to TATP. These methods rely on an array of sensors that change color upon exposure to TATP vapor. Specifically, one group has filed a patent [24] that utilizes the reaction of mineral acids to decompose TATP to hydrogen peroxide which then reacts with a peroxidase substrate that consequently acts as the colorimetric sensor. While incredibly selective, this colorimetric mechanism can take up to 5 minutes for detection [25] and thus is not a fast enough method to be employed by security systems.

Sensors employing conductometric techniques that measure conductance changes as explosive analyte comes in contact with a sensor are also being investigated [26]. This technique is similar to the methods used by our group in that a reference sensor is employed alongside an active sensor such that differential signal processing takes place to identify energetic molecules in the vapor phase [3]. This differential process is different than ours in that the reference sensor is exactly the

same as the active sensor yet this reference sensor only “sees” clean, uncontaminated air flow to be compared with the active sensor that is interrogating ambient air. Our group’s reference sensor “sees” the same ambient airflow as the active sensor however our reference sensor is uncatyzed and therefore unreactive to explosive molecules of interest. This will be further highlighted and explained in Chapter 3.

As mentioned earlier, x-ray imaging is utilized in CT tunnels for the identification of explosive compounds. Recent advancements have been made to CT tunnels such that solid explosives can be highlighted in a separate color by the CT tunnel itself [27]. Algorithms based on x-ray beam attenuation and object density, identify items within luggage of a similar density to known explosives. An example of this is shown below in figure 3 [27].



Figure 3: (top) photograph of what seems to be typical luggage. (bottom) CT image of the same luggage as above. The doll in the top image is an IED containing explosive that is highlighted in red by the CT image below [27].

While this new technology is great for identifying high density explosives, it has difficulty detecting low density explosives such as TATP. This is because the effective atomic number for the penetrating x-ray energy range of interest for TATP lies between some very common substances that are allowed to be carried on airplanes [28]. For comparison purposes, the effect atomic number for penetrating x-ray energy range of TATP lies between sugar and PMMA, a very common plastic. Another problem that makes TATP difficult to detect by this technique arises due to the fact

that TATP density, and thus effective atomic number for the penetrating x-ray energy range, can change dramatically based on how TATP is synthesized [28].

The current state of the art for TATP explosive detection is a trained bomb sniffing dog. Thanks to the high vapor pressure of TATP, if trained effectively, dogs are able to detect TATP vapors with great sensitivity and with directionality. Dogs do have a few drawbacks however: they require months of training, a handler at all times, and can become fatigued throughout the day. Not all dogs are able to complete explosive detection training programs and thus some time is wasted in identifying which dogs are suitable to be effective detectors. Dogs can also be significantly expensive to maintain if you factor in their needs for food and grooming.

Chapter 2.5: The Need for a Portable Electronic Dog Nose

All of the aforementioned explosive detection technologies have their own drawbacks in terms of sensitivity and upfront/maintenance costs that make the detection of TATP impractical in public venues. Therefore, there is a tremendous need for an explosive detector that is portable, extremely sensitive, selective, and inexpensive to maintain and operate in public venues that have the potential to be targeted by explosive terror attacks. Specifically, an explosive detector for TATP vapors is sorely needed.

The Department of Homeland Security is currently planning on spending over \$50 million in 2018 to develop new technologies for the detection of chemical, biological, and explosive detection equipment and over \$250 million in the procurement of explosive detection devices [29]. While DHS may be able to spend a

significant amount of money on explosive detection equipment, not all densely populated civilian venues have that luxury. Concert halls and sports stadiums often have to depend on their own private funding to account for security measures to defend the public from terroristic threats. This often leads to cheap security measures and often times no bomb detection technology at all, due to the extremely high cost of explosive detection equipment.

Chapter 2.6: Metal Oxidation and Reduction Reactions

The hypothesis presented in the following section is deeply rooted in metal oxides and their transition from one oxidation state to another. The sensors developed in the Sensors and Surface Technology Partnership (SSTP), utilize a sputtered metal oxide as an active catalyst used to detect the presence of explosives. Most of the sputtered metals are transition metals or post transition metals that have a number of stable oxidation states. The oxidation of a metal occurs from the tendency of compounds to fill their valence shells and satisfy electron pairs, thus forming a more stable compound [30]. Metals are able to fill their valence shells by reacting with species that have a tendency to give up electrons to satisfy their orbitals such as oxygen or fluorine. For the purposes of this investigation, the strongest oxidant present is oxygen and thus, the reaction between transition metals and oxygen will be the focus of this investigation. When exposed to certain environments, such as specific temperatures or reactive species, metal oxides can revert to lower oxidation states or even convert to a pure metal in a process known as reduction.

Like all chemical reactions, energy in the form of heat is consumed or released depending on the nature of the reaction. Exothermic reactions give off heat while endothermic reactions require heat to occur. All processes related to the oxidation of metals result in exothermic reactions and thus, the opposite process, reduction, is endothermic in nature [31-34]. Assuming all products and reactants are at the same temperature, the nature of exothermic and endothermic reactions is solely dependent on the difference in enthalpies of formation of reactants and products such that the heat of reaction is equal to [31]:

$$\Delta H_{rxn} = \sum v_p \times H_f(\text{products}) - \sum v_r \times H_f(\text{reactants})$$

Where:

ΔH_{rxn} = Heat of the reaction

v_p and v_r = stoichiometric coefficients for products and reactants respectively

H_f = Enthalpy of formation of the product or reactant

A positive ΔH_{rxn} indicates that the chemical system gained energy, thus the surroundings area had to supply this energy in the form of heat, resulting in an endothermic reaction. A negative ΔH_{rxn} indicates that the chemical system loses energy, resulting in a release of heat from the system, and an exothermic reaction [31]. The heat released or consumed by these oxidation or reduction reactions in the catalyst is how the thermodynamic sensor developed in the SSTP at URI operates.

Chapter 2.7: Previous URI Explosive Vapor Sensor Work

The use of metal oxide catalysts for the detection of explosive vapors was initiated in 2012 and was part of an ongoing investigation funded by the Department

of Homeland Security. The thermodynamic sensor platform has undergone extensive field testing in an attempt to expedite its use in a real world scenario.

Mallin [3] added a pre-concentrator to the thermodynamic sensor platform so explosive vapor could be collected semi-continuously and then release vapor all at once to send a burst of highly concentrated explosive vapor to the sensors. An example of this pre-concentration technique is shown below in figure 4.

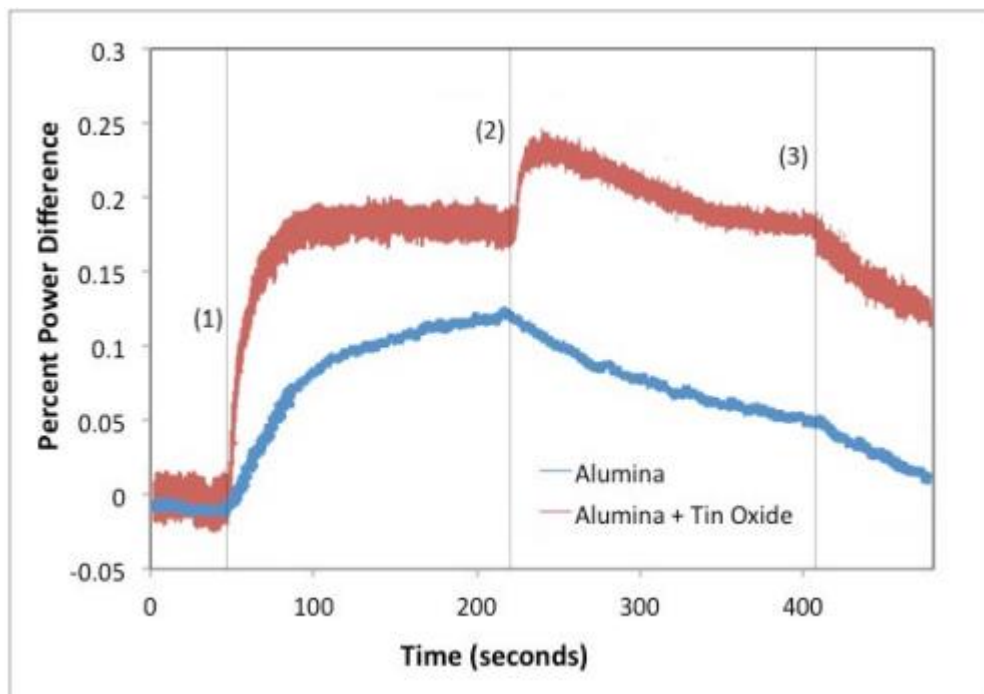


Figure 4: Preconcentration test conducted using a stoichiometric SnO₂ catalyst and 2,6-DNT using the dynamic control method: (1) beginning of DNT delivery to sensors (2) preconcentrator begins thermal desorption (3) preconcentrator is turned off and reference gas is reintroduced to the chambers [3].

Mallin [3] also proposed adding a conductometric sensing platform on the same substrate as the microheater for added sensing orthogonality to the pre-existing thermodynamic sensor. This conductometric platform utilized interdigitated fingers deposited on top of the metal oxide catalyst to interrogate the metal oxide for electrical

conductivity changes as the catalyst is exposed to the analyte. Typical orthogonal sensor responses are shown in figure 5.

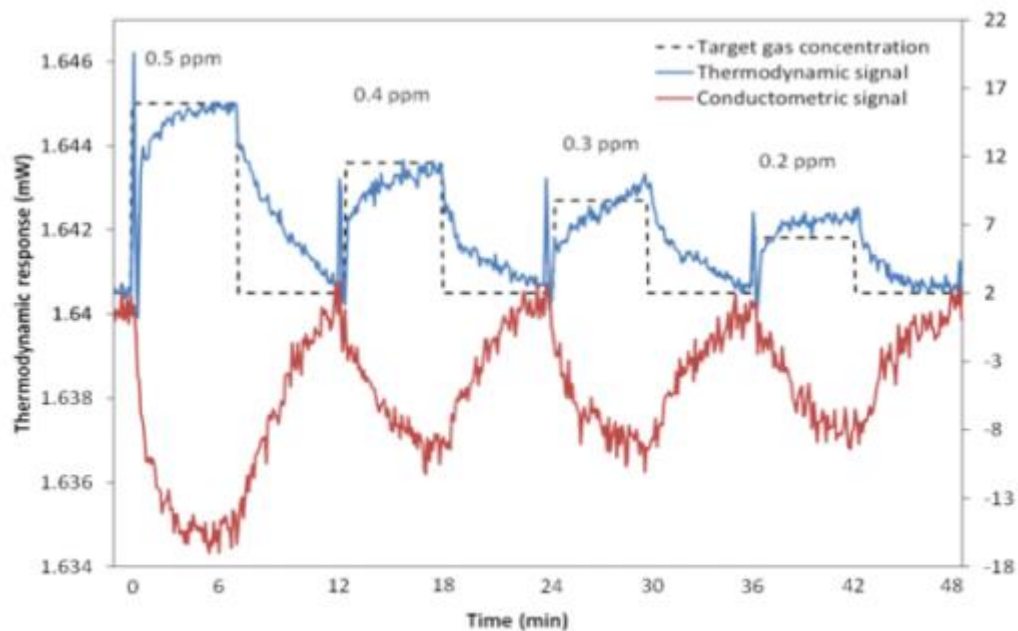


Figure 5: Orthogonal response of a tin oxide catalyst to 2,6-DNT vapor. Thermodynamic signal is shown in blue while the conductometric signal is shown in red [3].

Caron [2] produced 3D microstructural supports for the catalyst onto which the catalyst was sputtered in an attempt to increase catalytic surface area. This increase in catalytic surface area increased sensor sensitivity and thus, a lower detection limit was achieved. The response of a sensor with increased catalytic surface area is shown in figure 6.

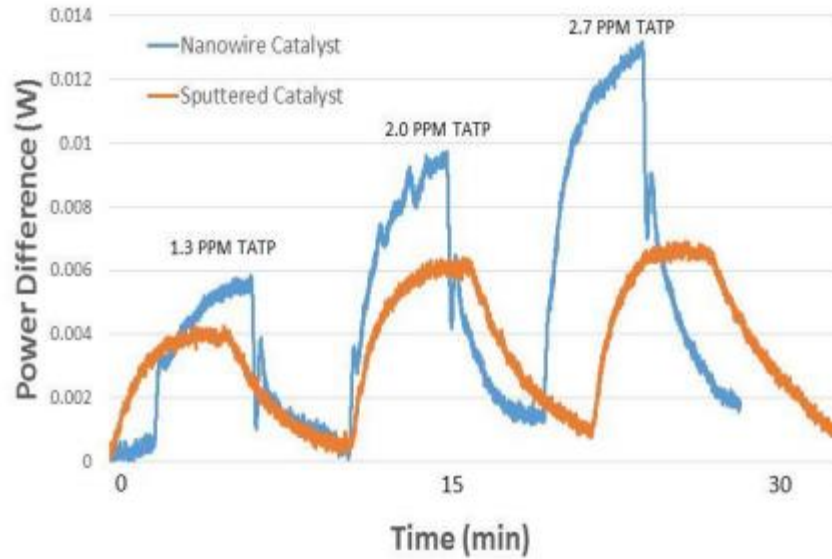


Figure 6: Tin oxide sensor responses to varying TATP concentration. Sensors are operating at 500°C. The orange response curve is from a sensor using a flat, as sputtered catalyst and the blue curves employ a sensor with nanowire catalyst supports to increase catalytic surface area [2].

Gomes [1] also focused on increasing sensor sensitivity. This was accomplished by changing the sensor platform altogether. Originally, the sensor utilized a microheater that was sputter deposited onto an aluminum oxide substrate. However, Gomes [1] proposed that the sensor employ a nickel coil microheater, which had a significantly lower thermal mass than the sputtered microheater. The decrease in thermal mass of the sensor greatly increased sensitivity to explosive heat effects, and larger responses to the same concentration of TATP analyte (figure 7).

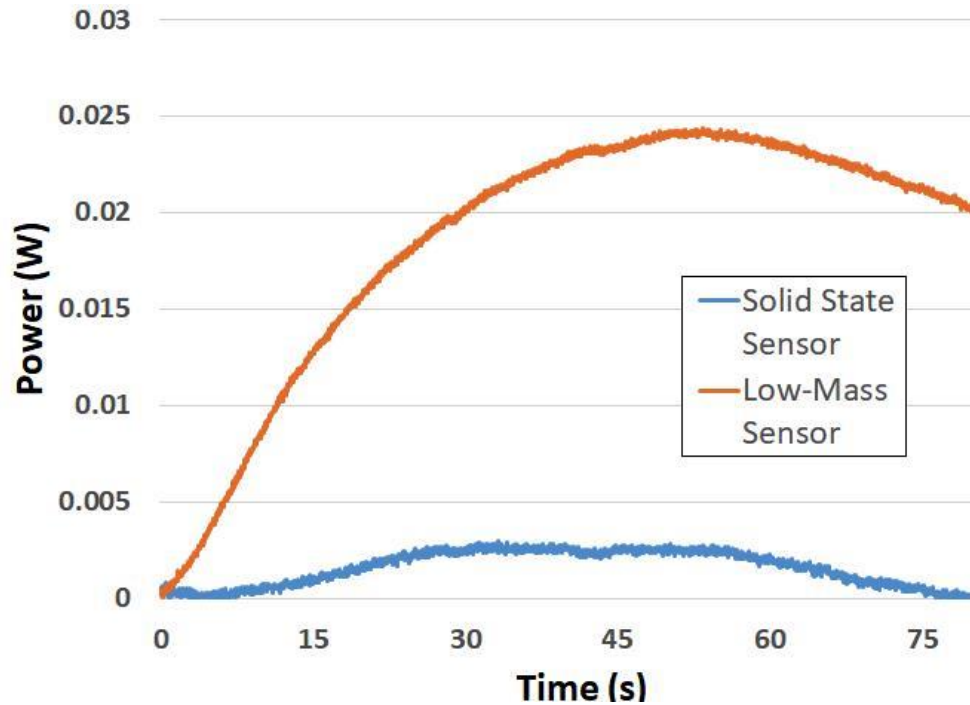


Figure 7: The difference in sensor platform sensitivity is highlighted here by the difference in responses from the substrate using microheater on an alumina substrate (blue curve) and the free standing low mass nickel microheater (orange curve). Both sensors used the same tin oxide catalyst, were exposed to the same concentration of TATP (20ppm), and were held at the same operating temperature (500°C)

Advancements made by Mallin [3] and Caron [2], while valuable, were not utilized by Gomes [1] for several reasons. First, for the sensor to operate in a continuous manner, the pre-concentration technique could not be used because it required sampling to be interrupted in order to replace the pre-concentrator after several hours of use. The conductometric platform used by Mallin [3] was sputter deposited onto a flat alumina substrate. However, once a nickel “coil” microheater replaced the thin film microheater deposited on the alumina substrate, the patterning of thin film leads onto the catalyst was not possible. The switch to the coil microheater also made the growth of 3 D microstructures incredibly difficult due to the fragility of

these structures and the tendency of the coil microheater to expand and contract upon heating and cooling processes.

CHAPTER 3

METHODOLOGY

Chapter 3.1: Sensor Fabrication

The sensor utilized for this research employed extremely low mass, freestanding nickel coils manufactured by HPI Inc., Ayer, MA. These microheater sensors monitor the heat effects in the metal oxide catalyst when exposed to the analyte and are a direct result of the catalyst–analyte interaction. The electronic trace detection (ETD) system employs two microheater sensors that are heated to predetermined constant temperature set points using VM heater software. VM heater utilizes an Anderson Loop for extremely fast and accurate measurement capabilities. The temperature of each sensor is induced through electrical resistance heating. Before heating, the resting resistance of each sensor is recorded, and based on the sensor’s thermal coefficient of resistance (TCR), a current traveling through the microheater is increased, thus causing the resistance of the microheater to increase, and consequently increasing the sensor temperature. The power required to maintain this constant resistance is monitored in real time using a laptop via a VM heater software window. This power is also simultaneously compiled into a text file so that it can be accessed in the future for further examination.

The microheaters were comprised of two copper electrodes, and a 25 μ m diameter nickel wire that was coiled and welded to the electrodes. The electrodes were soldered into D-subminiature 9 pin connectors (DB9 connectors) that allow for communication between the nickel microheater and the VM heater software. Once

soldered into the DB9 connector, the sensor is connected into a hole that has been cut into the side of a hollow, 1 inch diameter, PVC tube such that the microheater is centered in the tube. A photograph of this coil microheater (before mounting in the DB9 connector and PVC tube) is shown below in figure 8.

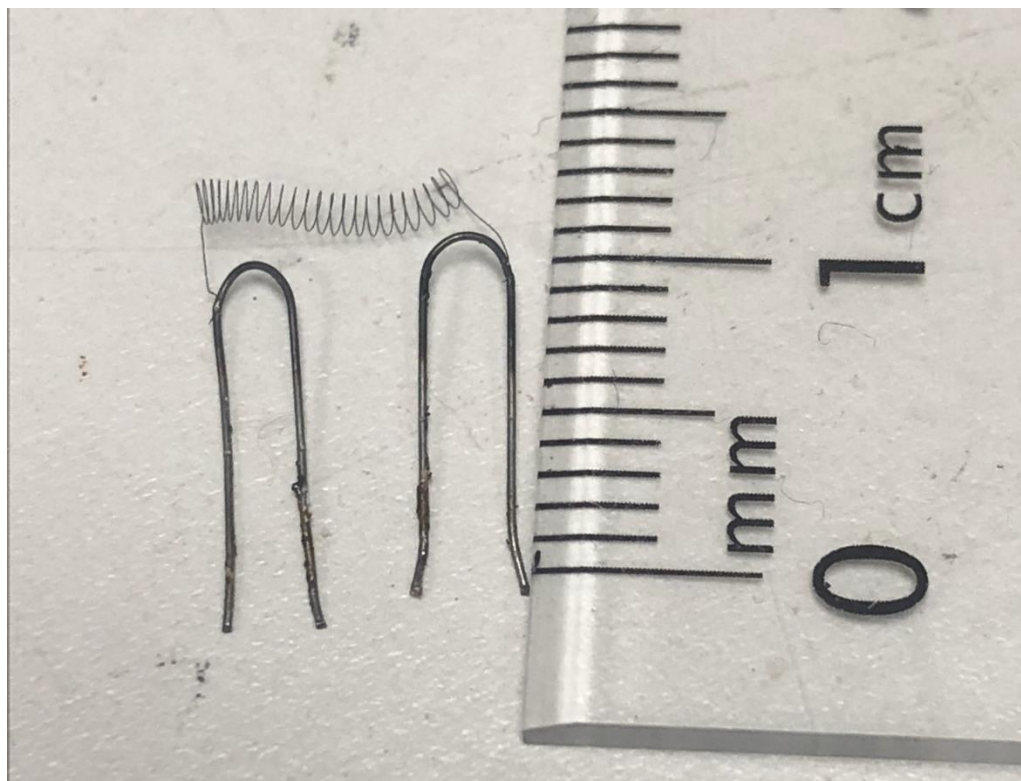


Figure 8: Nickel coil used as a microheater in the sensor platform.

The ETD system employs two microheaters at all times for differential signal processing. One sensor is coated with a metal oxide catalyst and the other is uncoated and used as a reference. Analyte such as TATP, exhibit a heat effect by interacting with the metal oxide catalyst. The reference sensor is used to subtract those heat effects that may arise due to less specific, non-catalytic, sensible heat effects, such as temperature changes of the incoming vapor stream.

Catalytically active sensors are coated with a metal oxide film deposited by RF sputtering. These oxide films were approximately 1 μm thick, however in certain areas this thickness may vary due to the fact that the microheaters must be sputtered twice, once on each side, to ensure complete coverage. Several oxides were used for catalyst preparation including CuO, SnO, ZnO, and FeO. Sputtering targets, measuring 6 inches in diameter, were used for catalyst deposition. All oxides were sputtered in a pure argon atmosphere at 7mT pressure and forward voltages of 900 V were used to sputter the metal oxide catalysts.

Chapter 3.2: Apparatus and Experimental Procedure

A typical test is conducted inside the SSTP laboratory using dry air as a carrier gas to deliver TATP vapor downstream to the sensor units. Dry air from an air tank is introduced to the ETD set up and travels downstream to the two sensor elements. There are 4 Alicat Scientific Mass Flow Controllers (MFCs) used in this testing apparatus: the first two are used to control whether the air stream flows into an empty chamber or a chamber containing analyte vapor, while the other two MFCs are used downstream to split the incoming airflow equally to each sensor. Flow rate to each sensor has been optimized at 130sccm to ensure the best combination of sensor sensitivity and response time (see chapter 4 for optimization experiment).

During a standard test, both sensors are heated to a predetermined temperature set point using sensor resting resistance, VM heater, and the TCR of the sensor. Temperature set points vary depending on the test, and can range anywhere between room temperature and 500°C. Once the sensors are heated, air flows through the empty

chamber and downstream to each sensor element. The power required to maintain the constant temperature set point is monitored, and allowed to equilibrate in the dry air stream such that a baseline is established. Once a baseline is established, the upstream mass flow controllers divert flow from the empty chamber to a chamber containing 5-10mg of solid TATP. TATP vapor from the actively subliming solid TATP is then picked up by the dry air carrier gas and sent downstream to the sensor elements. The MFCs used to divert carrier gas from the empty chamber to the TATP chamber are controlled by software known as Flow Vision. A schematic of the testing setup is shown below in figure 9.

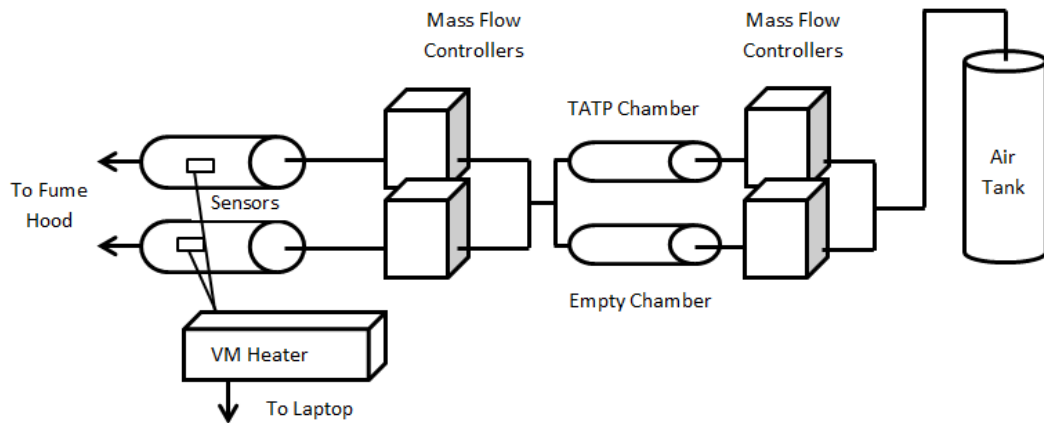


Figure 9: Schematic of the testing apparatus used in the testing procedures described

When TATP interacts with the catalyzed sensor either an endothermic or exothermic heat effect occurs depending on the catalyst and sensor temperature. An endothermic heat effect causes heat to be pulled from the sensor and thus VM heater acts to maintain the constant temperature set point by supplying extra power to the sensor. For exothermic heat effects, less power is needed to maintain the temperature

set point because of the energy supplied from the catalyst-analyte interaction and thus VM heater sends less power to the sensor.

Chapter 3.3: “Portable” Trace Electronic Detection System

A separate testing apparatus has also been constructed in an attempt to test for TATP vapors in real world environments under more realistic conditions such as temperature fluctuations and humid conditions. Instead of dry carrier gas being fed to the ETD system by a pressurized air tank, a Buck Libra Air Sampling Pump is used to suck ambient air into the system to be pushed to the active sensor elements downstream. Through the use of this pump, TATP can be introduced to the system by placing a vial of solid TATP in front of the pump inlet, such that the headspace vapors (not the solid TATP) from the vial are sucked into the system. There is no longer a need to use MFCs to divert airflow into a separate TATP chamber, however 2 MFCs are still used to split the airflow evenly between the two sensor elements. A mixing chamber located directly after the air pump is used to eliminate flow discrepancies that may arise from the pump’s air sampling behavior.

The same VM heater hardware/software is used to heat the sensor elements as the lab scale apparatus and the same laptop is used to heat and monitor power changes to the sensors. The entire portable testing setup (except for the laptop) is condensed and fit into a 14x14x21inch toolbox. The toolbox has been modified so that holes for the air pump inlet and sensor exhaust ports have been cut. Also, a small fan is placed in the box (not near the sensor elements) to cool off any electronics. A power supply for the VM heater electronics and MFC is still needed to make the apparatus truly

portable, however for testing purposes, a 5 outlet power strip is connected to an external power source. A schematic of this system is shown below in figure 10.

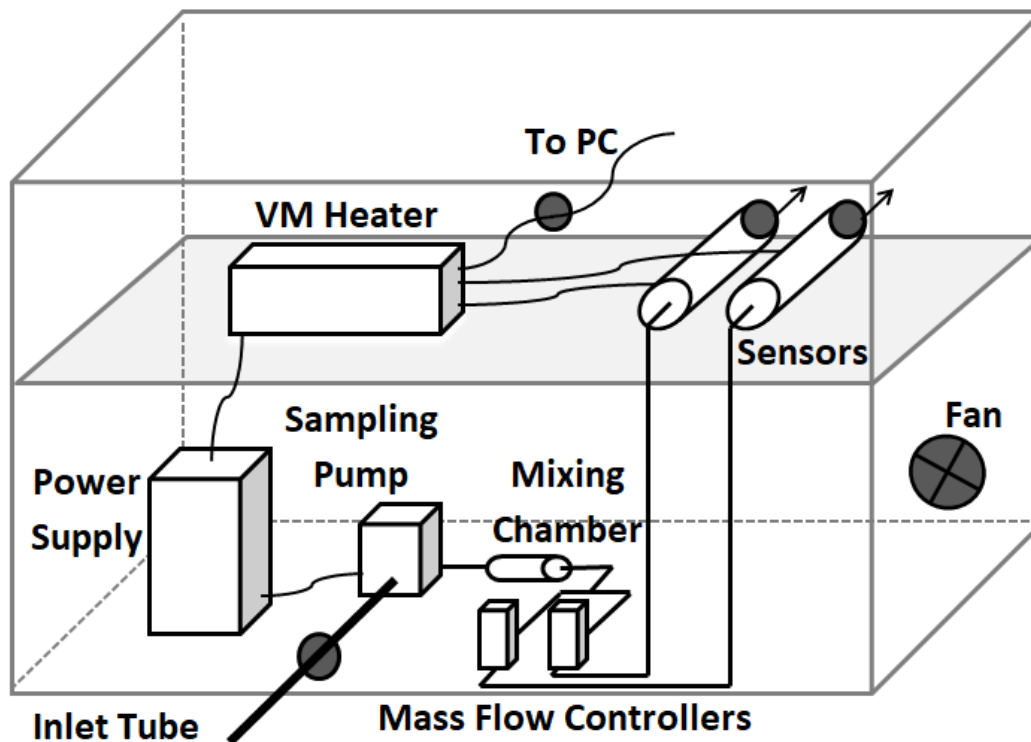


Figure 10: Schematic of the portable ETD system. A power supply is still needed to complete the ETD system however in order to test the apparatus, a power strip connected to an external power source has replaced the power source shown in the schematic

While most testing was done using the lab setup, select tests were performed using the portable system, such as flow rate optimization and humidity tests. Humidity tests were performed by introducing a 1000mL flask to the inlet tube such that ambient air was sucked into the flask, and then into the portable ETD system. Humidity could be controlled by adding 100mL of water to the flask, and heating the flask using a hot plate to bring the water just below boiling temperature. The heating of the water promoted evaporation and thus the headspace of the flask was considered to be at 100% relative humidity(RH). TATP vapor traveled through the flask and

mixed in the remaining 900mL of 100%RH headspace vapor before traveling downstream to the active sensor elements.

CHAPTER 4

RESULTS

Chapter 4.1: Portable System Testing

Chapter 4.1.1: Humid Environment Testing

Humidity was investigated as a primary interferent for the detection of TATP. Relative humidity levels ranging from 30%RH to 100%RH were systematically investigated using SnO₂ as a catalyst when detecting TATP. Using our portable detection system, the humidity level of the incoming vapor stream was controlled by the introduction of a 1000mL flask to the inlet tube as described in chapter 3.2. The headspace above the flask containing 100mL of a water was humidified by heating the water using a hot plate. Figure 11 shows that an increase in the relative humidity level (to 100%RH) substantially lowers the response to TATP, when SnO₂ was used as the catalyst to detect TATP. The red curve illustrates the response of the portable detection system with no water in the 1000mL flask while the green curve represents the response to TATP in a 100%RH environment. The diminished response likely occurred due to water molecules blocking catalytic sites on the SnO₂ surface, resulting in less interaction between the energetic material and metal oxide catalyst, and thus a smaller sensor response.

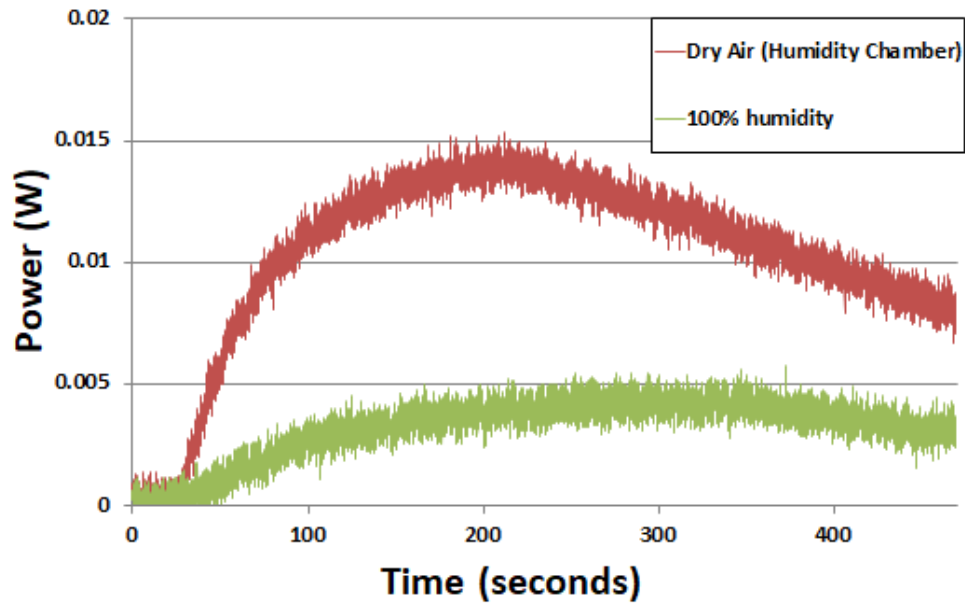


Figure 11: SnO₂ catalyzed thermodynamic sensor response to TATP under various conditions of humidity. Installing an empty vessel downstream from the TATP introduced a dilution effect (red curve), which lowered the response significantly compared to the portable ETD system operating using no flask.

Chapter 4.1.2: Nitrogen Annealing

This humidity effect does not simply disappear once the sensor is removed from the humid environment, but instead the effect is cumulative and greatly affects sensor performance even under dry conditions run shortly after humid environment experiments. Due to the cumulative effect of humidity, a nitrogen annealing process was developed in order to regenerate the catalyst and return the catalyst to its original state. Figure 12 shows the effect of nitrogen annealing on the regeneration of the catalyst and how the the sensor response was returned to its unaffected state. The red curve in Figure 12 is the response of a SnO₂ catalyst to 2.8 ppm TATP after a few hours of testing in 100%RH. It shows that the response to TATP is almost undistinguishable from the noise floor. After the catalyst was heated in dry nitrogen for approximately 15 minutes at 500C, the response returned to values prior to

humidity testing (blue curve); i.e. after heating in dry nitrogen, the sensor was rerun and the response increased significantly in comparison with the previous test.

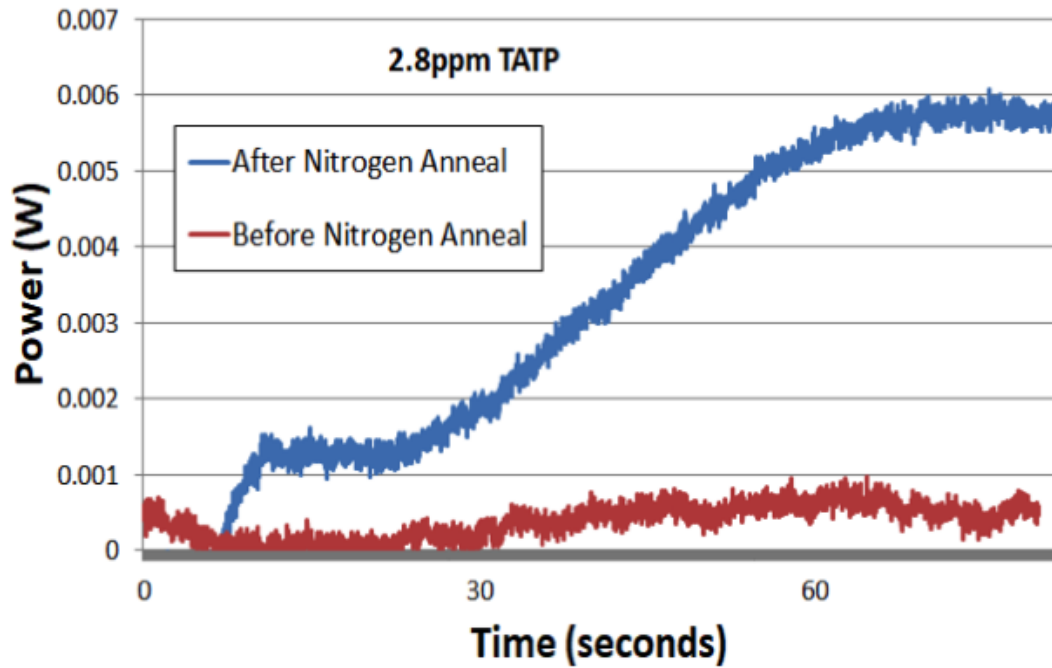


Figure 12: Effect of nitrogen annealing on a SnO₂ sensor when exposed to 2.8ppm TATP. Red curve represents sensor response after hours of testing in relatively high humidity conditions.

Chapter 4.1.3: Flow Rate Optimization

An investigation into the optimum flow rate for portable sensor detection was conducted by varying the flow rate to each individual sensor using the MFCs. Flow rates of 25, 130, 170, and 210 standard cubic centimeters per minute (SCCM) were individually tested and plotted below in figure 13.

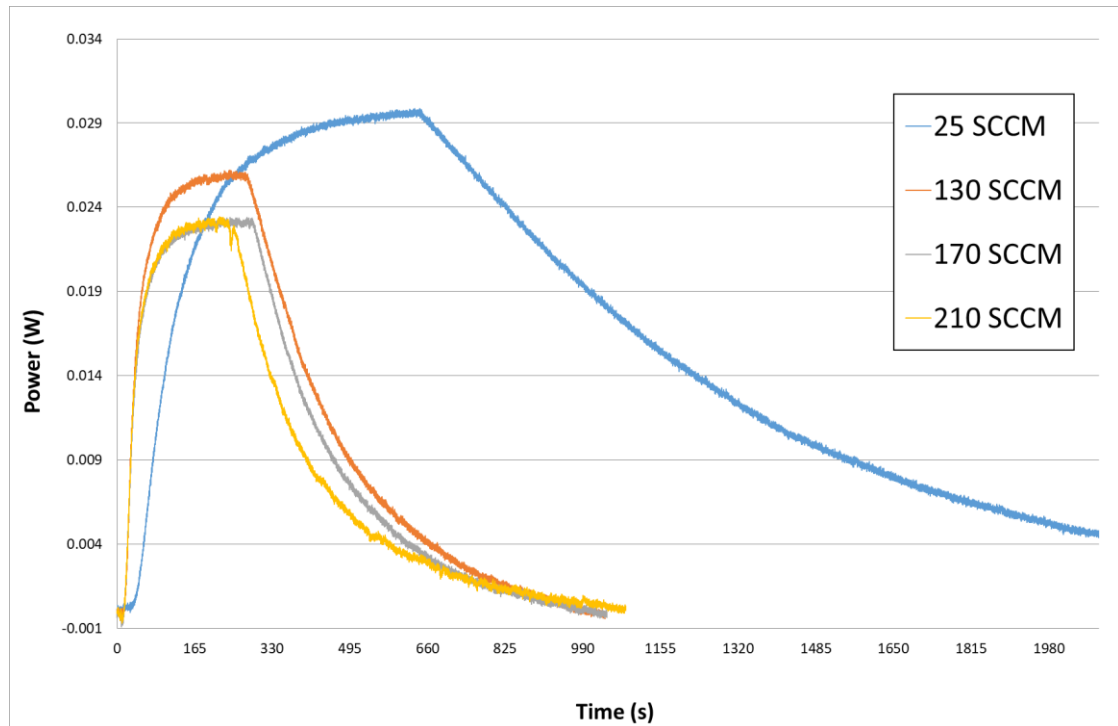


Figure 13: Sensor responses to 20ppm TATP utilizing a SnO sensor operating at 500°C. Flow rates of 25, 130, 170, and 210 sccm were investigated.

According to these tests, increasing flow rate to the sensor actually decreases the response to the same concentration of explosive vapor (20ppm TATP). This is most likely due to the increase in flow rate causing a cooling effect on the sensors, shrouding the endothermic heat effect that occurs from SnO-TATP interaction at 500°C. This cooling affect prompted decreasing responses from 25-170sccm but no decrease in sensor response occurred at flow rates higher than 170sccm. While 25sccm may be the flow rate that the sensor is most sensitive to TATP vapor, it also has a significantly slower response time compared to 130, 170, and 210sccm. At 25sccm it takes approximately 700 seconds for sensors to reach their maximum power change as opposed to 250 seconds for the other three flow rates. This severe difference is due to the rate at which explosive vapor is able to diffuse through the portable ETD system

and to the PVC tube housing the sensor components. From this experiment, it was noted that the optimal sensing flow rate is 130sccm because that is the flow rate at which sensor response time is quickest and there is minimal cooling affects that diminish sensor sensitivity.

Chapter 4.2: Detection Mechanism

Chapter 4.2.1: Oxidation and Reduction of Tin Oxide Catalysts

The thermodynamic sensor was able to detect explosives at trace levels with unprecedented accuracy. Lower detection limits have been achieved due to the improved sensitivity of the low thermal mass sensor, and thus, it was possible to better understand the nature of the thermal response as the temperature was scanned between 50 and 500°C. Several seminal experiments have been conducted to establish a mechanism/pathway for the detection of explosives using the thermodynamic sensor. It appears that the heat effects associated with detection rely heavily on oxidation-reduction reactions occurring on the surface of the metal oxide catalyst upon exposure to the explosive molecule. Figure 14 shows the response of the sensor employing a SnO catalyst to 20 ppm TATP at various temperatures. Each experiment was conducted according to the lab scale protocol described previously in section 3.2. The set point temperature established at the beginning of each run was varied from 130°C to 375°C. When the sensor was operated at temperatures of 275°C and below, an exothermic response to TATP was observed. However, at 375°C, a large endothermic response was observed when exposed to TATP.

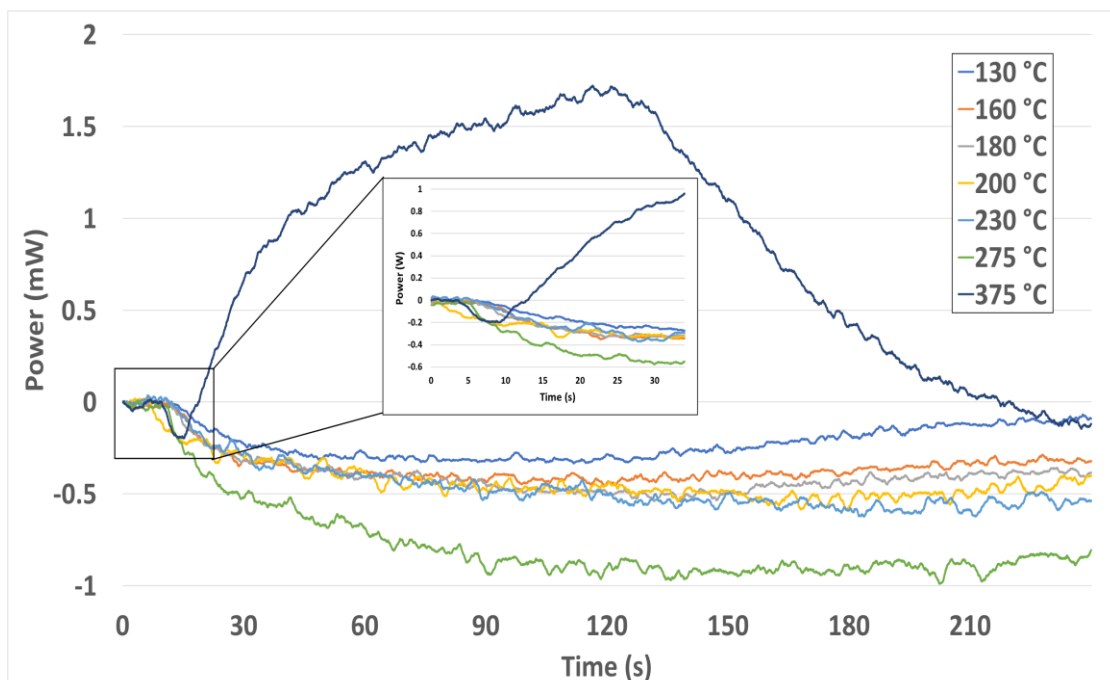


Figure 14: Sensor response of a SnO catalyst to TATP in air at varying temperatures. The inset figure highlights the first 30 seconds of the experiment where the sensor temperature of 375 °C initially responded exothermically, before a much larger endothermic heat effect was observed.

The metal oxide catalyst comprising the sensor was then subjected to a high-pressure oxidation treatment to convert the SnO (Sn^{+2}) to SnO₂ (Sn^{+4}). This oxidation treatment consisted of heating the metal oxide to 600 °C for two hours in 2atm of pure oxygen. The sensor was then exposed to TATP in a series of tests at various temperatures (identical to the procedure used to generate figure 14). The responses of the metal oxide catalyst after a high-pressure oxidation treatment are shown in figure 15. Unlike the responses shown in figure 14, the high-pressure oxidation treatment resulted in no exothermic responses upon TATP exposure but instead exhibited a large endothermic response at temperatures above 200 °C. At temperatures below 200 °C, no response to TATP vapor was observed, whereas at temperatures above 200 °C, the responses were largely endothermic in nature.

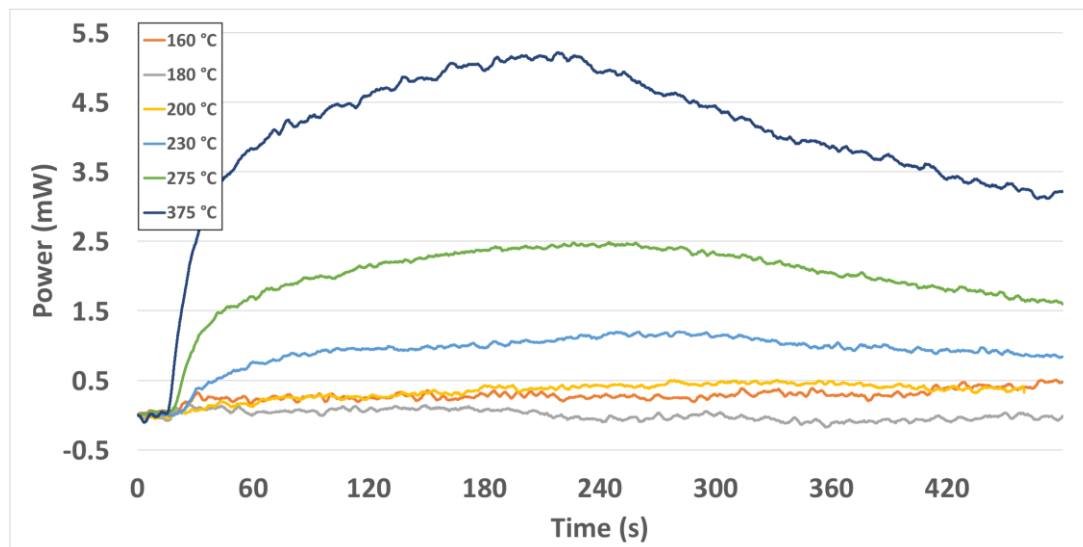


Figure 15: Sensor response of a SnO₂ catalyst to TATP in air at various temperatures.

It is believed that the exothermic response exhibited by the SnO sensor at low temperatures shown in figure 14 is due to the oxidation of SnO (conversion of Sn⁺² to Sn⁺⁴) in the presence of the explosive molecule (TATP) or its decomposition products. No exothermic response was observed using the SnO₂ catalyst prepared from the high-pressure oxidation treatment, since the metal oxide was already converted to its most oxygen rich state and thus, the catalyst could not be further oxidized. The endothermic responses exhibited by the conversion of SnO to SnO₂ were a result of catalytic decomposition of the TATP molecule and its decomposition products and the associated reduction of the oxide (reduction of Sn⁺⁴ to Sn⁺² or Sn⁺² to Sn). A closer look at the response of the sensor using a SnO catalyst shows that as the temperature increases, TATP is catalytically decomposed (inset of figure 14). These two heat effects appear to compete with one another until the endothermic heat effect dominates. Highlighted in the inset of figure 3, the blue curve represents the sensor response at a temperature of 375°C which initially exhibits an exothermic heat effect

associated with the lower-temperature sensor responses. After 20 seconds, the sensor begins to catalytically decompose the TATP and an endothermic heat effect was observed due to the specific decomposition products of the TATP analyte.

Additional evidence that the metal oxide-analyte interactions are attributed to oxidation/reduction reactions at the metal oxide surface was provided by an activation energy analysis. For a SnO_2 -TATP interaction, an activation energy was established and compared to the activation energy for the associated reduction of the metal oxide. A rate constant was established at each temperature, where an endothermic response was observed and plotted as a function of reciprocal temperature to establish an activation energy for the SnO_2 -TATP interaction. In this case, an activation energy of 16Kcal/mol was established for TATP detection using the SnO_2 catalyst, which is the same activation energy associated with the reduction of SnO_2 to SnO (conversion of Sn^{+4} to Sn^{+2}) reported by Kim et al [35], which was 15Kcal/mol.

Chapter 4.2.2: Oxidation and Reduction of Copper Oxide Catalysts

A series of similar experiments were conducted using Cu_2O and CuO catalysts instead of SnO catalysts were repeated and the resulting activation energy for the detection process using these catalysts was compared to the activation energy associated with the oxidation/reduction of the metal oxides. A microheater coated with a Cu_2O catalyst was exposed to TATP at various temperatures and the associated responses are shown in figure 16. Here, temperatures between 130°C and 230°C resulted in an endothermic response but at 275°C , an exothermic response was observed. Similar to the responses using SnO and SnO_2 catalyst coated microheaters,

it appears that the endothermic response using a Cu_2O catalyst was a direct result of the decomposition of TATP and the simultaneous reduction of the metal oxide (conversion of Cu^{+2} to Cu^{+1}) upon exposure to TATP.

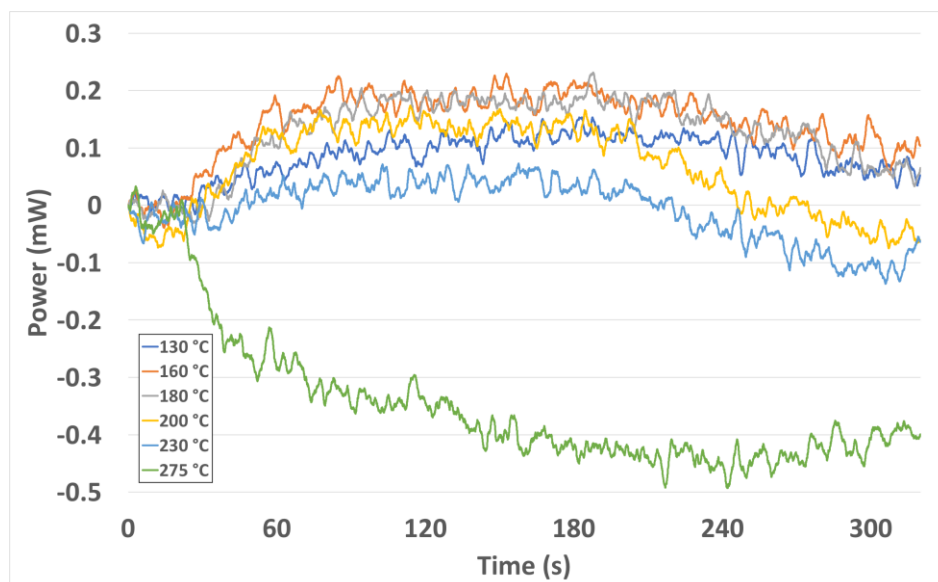


Figure 16: Sensor response of a Cu_2O catalyst to TATP in air at various temperatures.

After this Cu_2O temperature sweep, the same process used to convert the SnO to SnO_2 (convert Sn^{+2} to Sn^{+4}) was used to convert the Cu_2O to CuO (convert Cu^{+1} to Cu^{+2}). The curves shown in figure 17 were generated using a freshly oxidized CuO sensor. Here, no endothermic response to TATP was observed using the CuO catalyst at low temperatures. However, at higher temperatures both Cu_2O and CuO respond exothermically to TATP. Similarly, the exothermic response exhibited by the SnO catalyst at low temperatures, was due to the oxidation of the copper oxide (conversion of Cu^{+1} to Cu^{+2}). In an attempt to provide further evidence that these exothermic responses are due to the oxidation of the metal oxide, an activation energy based on the rate constant of individual exothermic response curves at different sensor temperatures (375-500°C) was calculated using a Cu_2O catalyst that was exposed to

TATP. The calculated activation energy was 8.0 Kcal/mol, which is similar to an activation energy of 9.6 Kcal/mol cited for the oxidation of Cu_2O reported by Zhu et al [36]. This further illustrates the unparalleled sensor selectivity with this detection system, in that TATP does not catalytically decompose to cause endothermic heat effect when subjected to certain oxidation states of copper oxide; e.g. CuO .

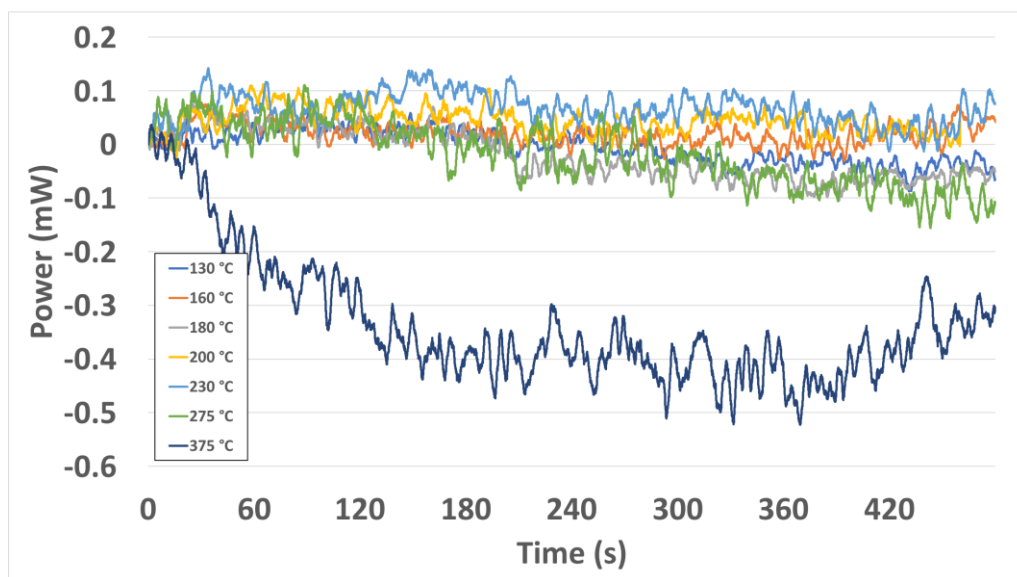


Figure 17: Sensor response of a CuO catalyst to TATP in air at various temperatures.

Chapter 4.2.3: Reduction of Zinc Oxide Catalysts

To confirm that the changes in sensor response using tin oxide and copper oxide catalysts were due to oxidation state changes that occur in the oxide catalyst after a high pressure-oxidation heat treatment, zinc oxide was also investigated as a catalyst. In a similar series of experiments, a catalyst-coated and uncoated microheater were cycled to different set point temperatures and the response was measured, similar to those shown in figures 14-17. The results of these thermal cycling experiments are

shown in figure 18. Zinc oxide (ZnO) was chosen here as the catalyst because there is only one oxidation state for zinc (Zn^{+2}) and thus, no oxidation state change was expected after a high-pressure oxidation heat treatment. Also, no exothermic reactions were anticipated after exposure to TATP. Figure 18 illustrates the response of the ZnO catalyst before heat treatment that was exposed to 20ppm TATP. At similar temperatures used for the tin oxide and copper oxide experiments (160-500°C), only endothermic responses to TATP were observed. After the high-pressure oxidation treatment, the ZnO catalyst-coated sensor exposed to TATP exhibited endothermic responses at all temperatures to TATP, similar to the behavior observed for the experiments where SnO was converted to the higher oxidation state, SnO₂. The temperature sweep experiment for ZnO exhibited the same behavior before and after heat treatment in a high pressure oxygen atmosphere.

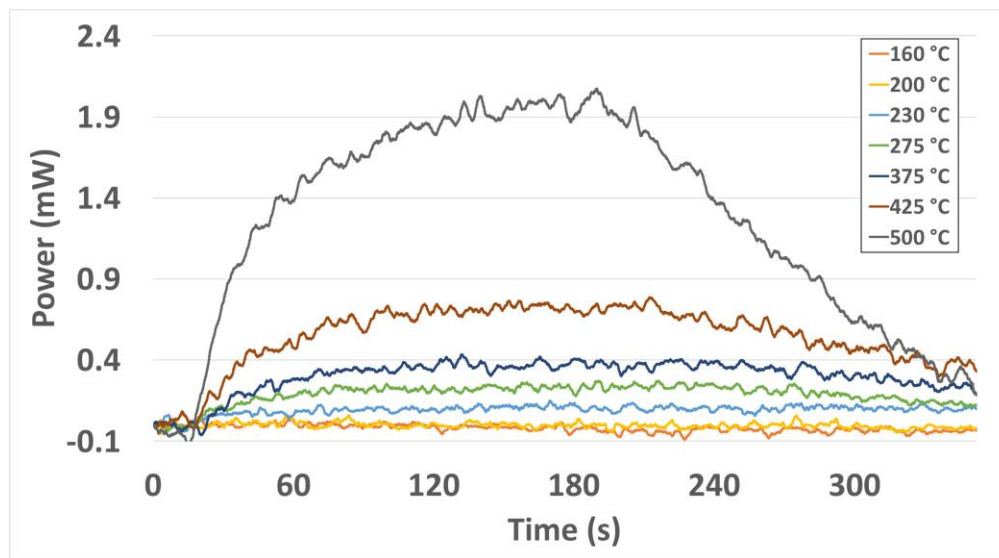


Figure 18: Sensor response of ZnO catalyst (before and after heat treatment) to TATP in air at varying temperatures.

To provide further evidence that the detection mechanism for our thermodynamic sensor is related to oxidation/reduction of the metal oxide used as a catalyst, an activation energy analysis was also performed for the case where ZnO was reduced as the temperature was swept from 160-500°C. Accordingly, the activation energy associated with our sensor response to TATP was approximately 19 Kcal/mol, which according to Lew et al [37] is not exact, but consistent with the known activation energy for the reduction of ZnO to Zn metal which is 24 Kcal/mol.

Chapter 4.2.4: SEM Confirmation

Figure 19 shows the fracture surface of a tin oxide coating deposited on a nickel microheater that was repeatedly driven from room temperature to 500°C. This image was taken by Gomes [1] during his research in 2016 however upon further investigation, it provides further evidence of oxidation state changes occurring on the surface of the catalyst. During thermal cycling, the tin oxide catalyst was exposed to TATP vapor. Here, the tin oxide surface exhibited relatively smooth rounded protuberances with minimal surface area, typical of an as-sputtered film. Also worth noting is that the tin oxide coating in figure 19 had separated from the substrate and developed small micro-cracks. Consequently a small gap was formed between the tin oxide and nickel substrate, which likely developed due to thermal stresses in the coating as a result of thermal cycling.

The columnar structure evident from the SEM fracture surface shown in figure 19, indicates that the tin oxide coating closest to the nickel substrate is slightly lighter in color compared to the outer layer of the coating. These SEM's were taken in

backscattered mode, where the contrast developed in the images is related to atomic number of the atoms comprising the coating. A bright area represents a more dense material and thus lower oxygen content (more metal rich area). Consequently, the darker outer layer in the cross section of the micrograph of figure 19 suggests that this material may contain more oxygen and less metal than the inner layer. This color gradient further suggests that as the tin oxide catalyst is exposed to TATP vapor, it changes oxidation state. A typical as-sputtered SnO catalyst that has not been exposed to TATP vapor would have an appearance similar to that of the innermost layer of the SnO catalyst shown in figure 19.

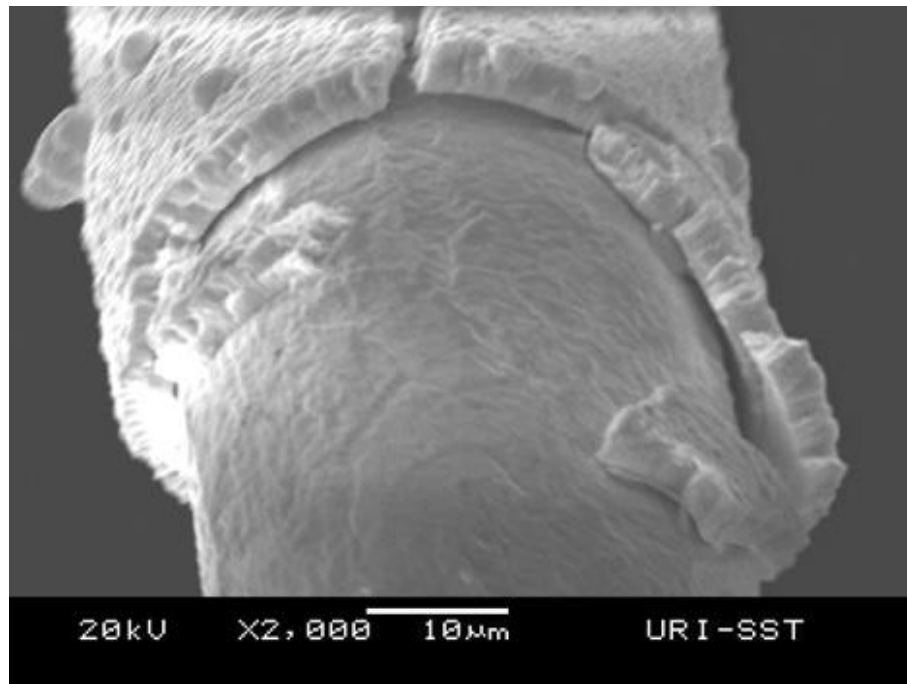


Figure 19: SEM fractograph of a nickel microheater coated with a SnO catalyst after exposure to TATP vapor.

Chapter 4.3 Improved Selectivity via Catalyst Selection

Sensor selectivity is still somewhat of a concern to reliably distinguish between different volatile compounds that may exhibit similar responses when exposed to the sensing platform. While TATP has been the main focus of this sensor research, other explosive compounds are also detectable using this ETD system, for example DADP, a decomposition product of TATP, as well as 2,4-Dinitrotoluene (2,4-DNT), a nitrogen based compound extremely prevalent in vapors emitted from solid TNT explosive. One concern for the detection of nitrogen based explosives such as 2,4-DNT versus peroxide based explosives such as TATP, is that nitrogen based explosives exhibit heat effects when exposed to uncatalyzed reference sensors.

This heat effect is highlighted below in figure 20. Here, 2,4-DNT vapor was exposed to the lab scale ETD system in the same manor that TATP is exposed for standard testing procedures. In figure 20, both the reference sensor (orange curve) and a SnO₂ catalyzed sensor (blue curve), heated to 375°C, are simultaneously exposed to 2,4-DNT. Both sensors endothermically respond to the 2,4-DNT vapor, illustrating that oxidation or reduction processes may not be the only heat effect associated with 2,4-DNT-sensor interactions. While the reference sensor does show significant response to these vapors, it is still very possible to distinguish between the reference sensor and the catalyzed SnO₂ sensor response and consequently, some catalytic interaction must be taking place.

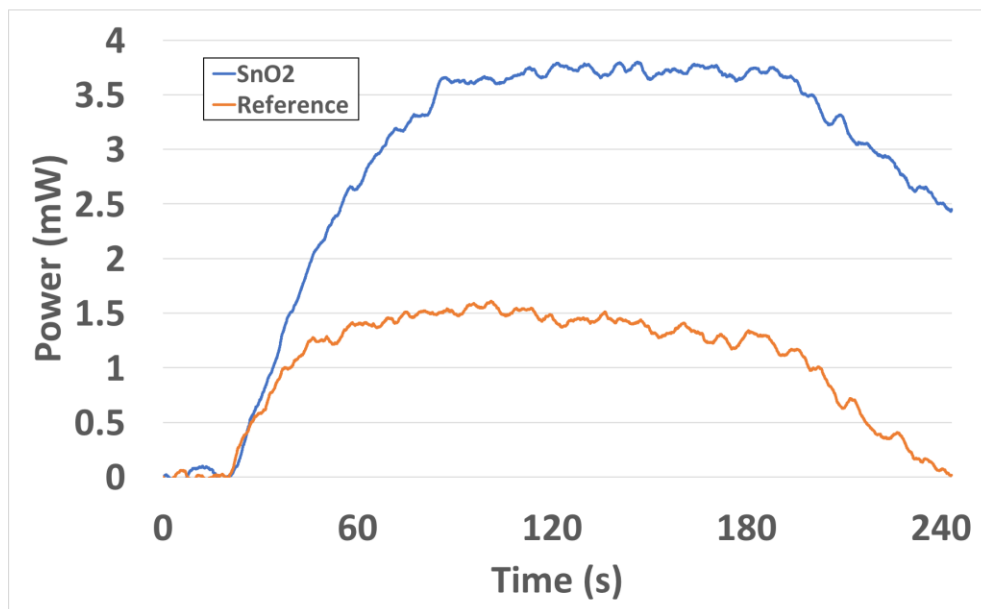


Figure 20: Catalyzed (blue) and reference (orange) sensor response to 2,4-DNT vapors. Both sensors are heated to 375°C and exhibit significant endothermic signals.

Unlike 2,4-DNT, the ETD system is very selective to peroxide based explosives such as TATP in that only the metal oxide catalyzed sensor will exhibit a heat effect while the nickel reference microheater will remain at a constant power level as it is exposed to the TATP vapor. This is illustrated in figure 21 where a similar experiment to that with 2,4-DNT was conducted, and both the reference sensor and catalyst sensor signals are plotted independently. No power change is exhibited by the uncatalyzed sensor while the SnO₂ sensor exhibits a 1.75mW endothermic response. Once again, both sensors were held at 375°C and exposed to 20ppm TATP for this experiment.

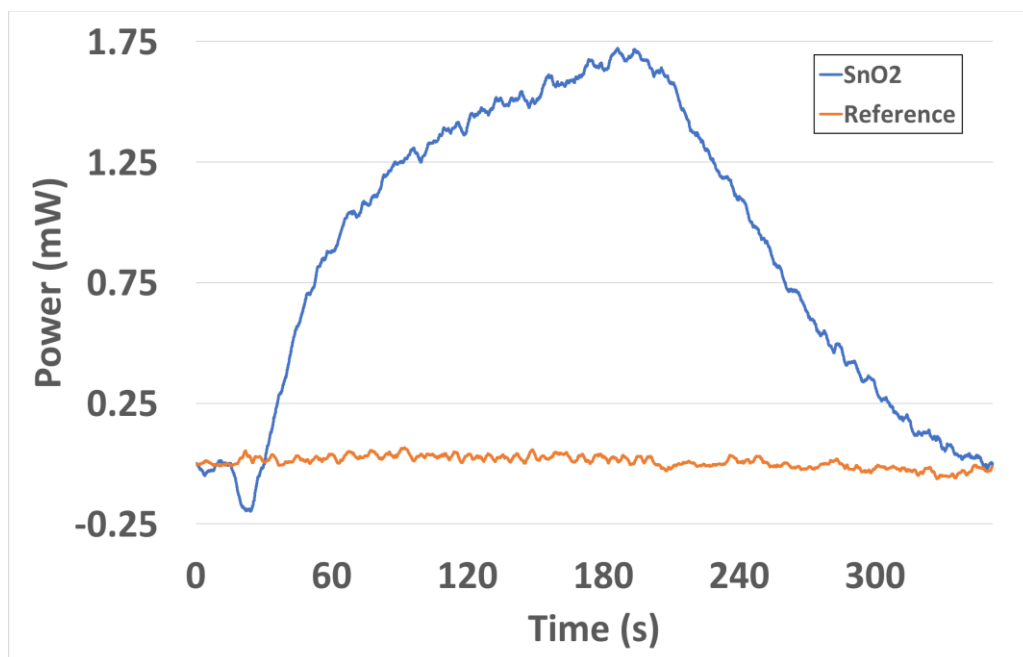


Figure 21: Catalyzed (blue) and reference (orange) sensor response to TATP vapor. Both sensors are heated to 375°C and only the catalyzed sensor exhibits a significant endothermic signal.

Both 2,4-DNT and TATP vapor display endothermic heat effects to a SnO₂ catalyst at the same temperature (375°C). While both compounds are dangerous, it would be advantageous to have a sensor that can distinguish between different volatile compounds. While this may be the case for SnO₂, not all catalysts exhibit the same behavior to the different explosive vapors. For this reason, characteristic “fingerprint” plots were constructed to differentiate between explosive compounds. Below in figures 22, 23, and 24, fingerprint characteristic curves for TATP, DADP, and 2,4-DNT respectively were produced. For these plots individual tests employing a SnO₂, ZnO, CuO, or FeO catalyzed sensor heated to 500°C, were exposed to the analyte of interest (TATP, DADP, or 2,4-DNT).

Each of these characteristic curves has their own unique features. For the TATP curves, SnO₂, ZnO, and FeO sensor responses were all endothermic in nature

while the CuO response was exothermic (figure 22). This curve was similar, but not identical to the curve of the TATP decomposition product, DADP. DADP exhibited endothermic responses to SnO₂, and ZnO and an exothermic response to CuO, however no response was observed to the FeO catalyzed sensor (figure 23). This shows that FeO catalysts are selective to TATP vapor but not for DADP vapor. The fingerprint curves for 2,4-DNT (figure 24) show that all four catalysts exhibit endothermic responses when exposed to 2,4-DNT vapor. Overall, each of these three plots are unique through the utilization of multiple different catalyst sensor responses.

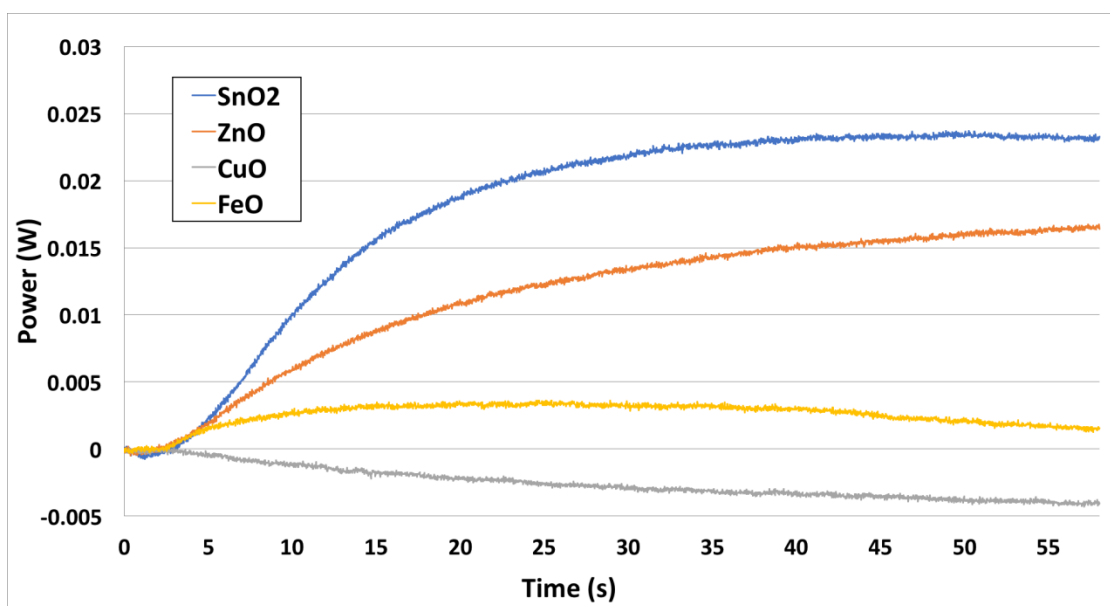


Figure 22: SnO₂, ZnO, CuO, and FeO sensor responses to TATP vapor at sensor temperatures of 500°C

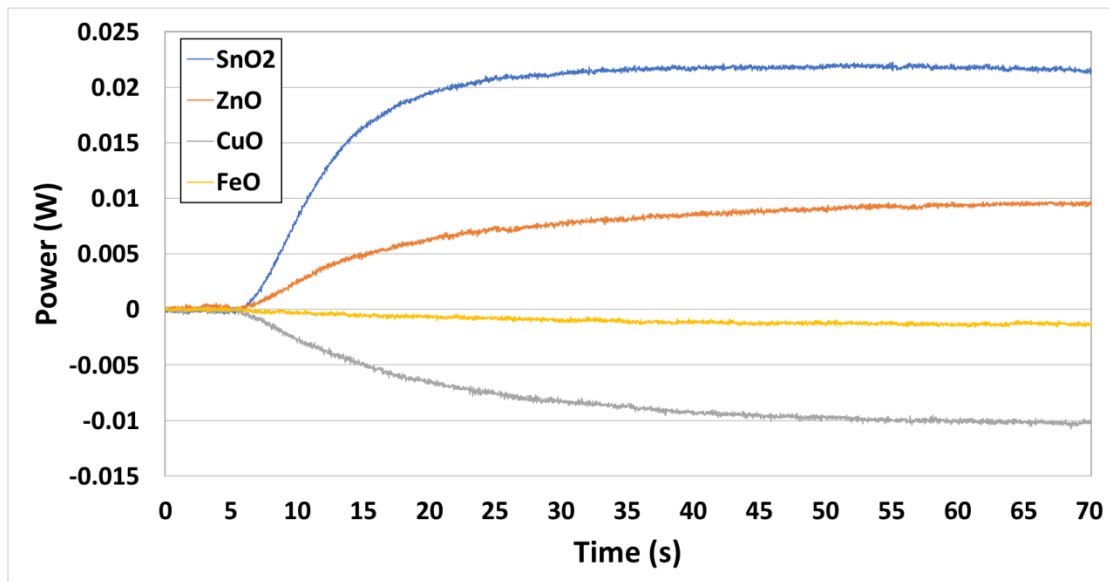


Figure 23: SnO₂, ZnO, CuO, and FeO sensor responses to DADP vapor at sensor temperatures of 500°C

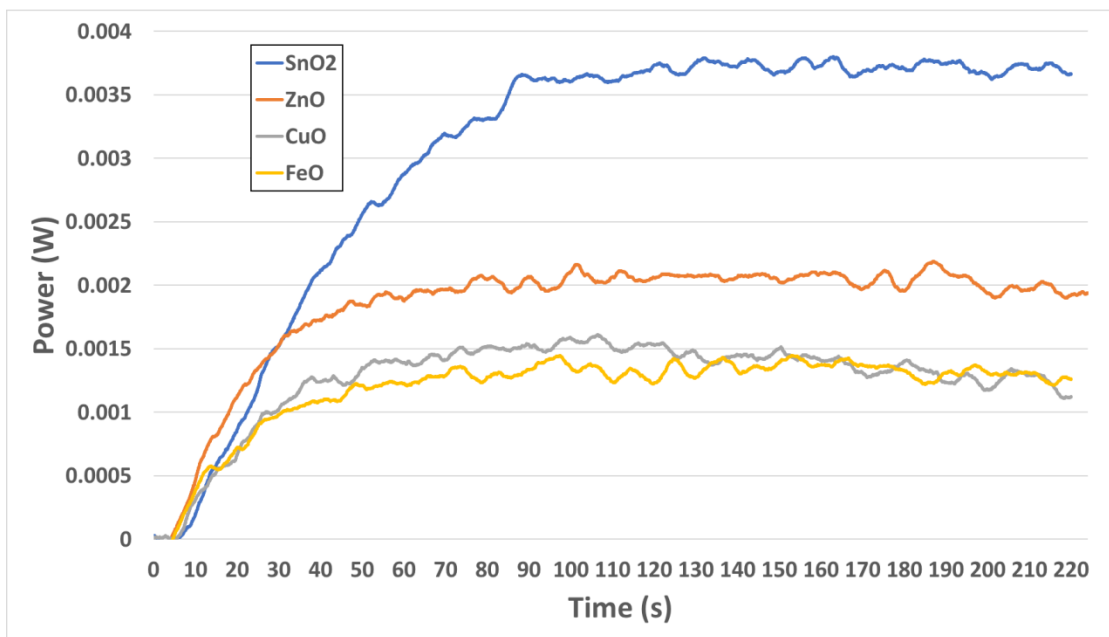


Figure 24: SnO₂, ZnO, CuO, and FeO sensor responses to 2,4-DNT vapor at sensor temperatures of 500°C

CHAPTER 5

CONCLUSION

Chapter 5.1: Conclusions

Due to the improved sensitivity of the thermodynamic sensor platform attributed to the reduction in thermal mass of the microheaters used for the thermodynamic sensor platform, the detection mechanism for this ETD system has been identified. The detection of explosives at trace levels relies heavily on oxidation or reduction of the metal oxide catalyst deposited on the microheater surface. Specifically, it relies on the decomposition products derived from the explosive and their interaction with the metal oxide. Metal oxides such as tin, copper, zinc, and iron oxides behave differently depending on the temperature at which the explosive decomposes. The observed sensor behavior is due to the available oxidation states of the metals mentioned above. Some metals have only one oxidation state such as zinc (Zn^{+2}), while others such as tin have multiple states (Sn^{+2} or Sn^{+4}). Metals having multiple oxidation states can be further oxidized or reduced depending on the nature of the decomposition products; i.e. a change in oxidation state will result depending on sensor temperature and the decomposition products and the associated heat effect is measured with exceptional sensitivity.

This oxidation/reduction mechanism has been confirmed in a series of seminal experiments whereby by a series of temperature sweep tests were conducted using tin, copper, and zinc oxide catalysts. Both tin and copper exhibited exothermic and endothermic heat effects over the temperature range of interest due to the availability

of multiple oxidation states. The tin oxide catalyst reverted to its most oxygen rich oxidation state using a high-pressure oxygen heat treatment and from there, no oxidation heat effects were observed upon subsequent temperature sweep tests. The same high-pressure heat treatment was performed on a copper catalyst, however the copper oxide did not revert to its highest oxidation state and thus, further oxidation was still possible when the copper oxide was subjected to high temperature exposure in the presence of TATP vapor. The zinc oxide catalyst exhibited only endothermic heat effects when exposed to TATP because zinc has one stable oxidation state and thus, the ZnO could not be oxidized further. The zinc oxide catalyst was subjected to the same high-pressure oxygen heat treatment as the tin and copper oxides and no changes in response behavior were noted over the same temperature range after heat treatment.

Activation energy calculations were performed for each of the three oxide catalysts investigated and were found to be consistent for oxidation or reduction reaction values reported in the literature. SEM imaging was also used to confirm the metal oxide catalyst is changing oxidation state at the surface where explosive analyte-catalyst interacts occur.

An investigation into sensor selectivity was also conducted in an attempt to categorize different explosives based on their behavior using different metal oxide catalysts. For example, nitrogen based explosives exhibit different heat effects even when exposed to the uncoated reference microheater, whereas TATP exhibited no heat effect. This suggests that thermal decomposition, not related to catalytic activity or catalytic decomposition, occurs when 2,4-DNT interacts with sensor.

Characteristic curves were generated for explosive vapors TATP, DADP, and 2,4-DNT. Each of these curves utilized FeO, SnO₂, ZnO, and CuO catalyzed sensors operating at 500°C. Due to the very specific interactions with individual catalyst-analyte pairings, the resulting curves will act as fingerprints or unique signatures that can be used to categorize explosive vapors for further testing.

Chapter 5.2: Future work

For increased sensor selectivity, more metal oxide catalysts should be investigated relating to how they interact to different explosive vapors. These metal oxide catalysts should be capable of jumping to multiple different oxidation states in order to produce the most unique sensor responses over a wide range of temperatures. Some metals that are capable of these oxidation state jumps are vanadium, chromium, and manganese.

Other peroxide based explosives such as HMTD should be investigated and their behavior compared to that of TATP. Additional fingerprint characteristic curves should be produced and cataloged for other explosive analyte and even for other volatile compounds that may trigger sensor responses. The utilization of these fingerprint curves could help mitigate false-positive responses to volatile compounds that may not exhibit explosive characteristics.

Additionally, in order to quickly and effectively utilize these fingerprint plots in real time testing scenarios, the ETD setup must be modified such that more than two sensors can operate simultaneously. Ideally, all four catalysts used in for these plots would operate together in an array format such as in the figure below (figure 25).

The largest difficulty that would be faced with this sensor array is isolating heat effects between sensors to ensure that the heat effect from one sensor has no influence on the sensor operating next to it.

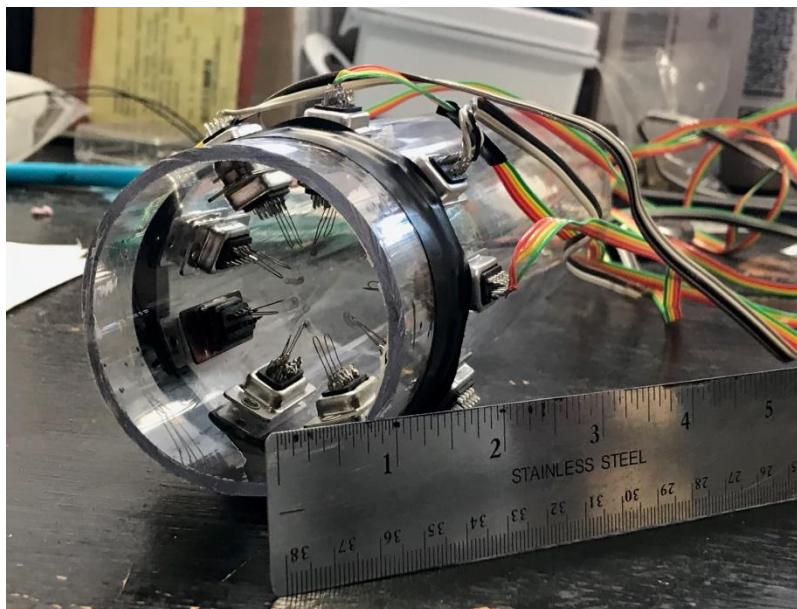


Figure 25: Modified sensor housing capable of holding up to 9 sensor devices at once.

Addition selectivity can be achieved by utilizing sensor catalysts that behave differently depending on their operating temperature. For example, Cu_2O and SnO catalysts behave both endothermically and exothermically between the operating range of 25-500°C. By varying the operating temperature of sensors such as these, an additional layer of selectivity can be incorporated into the ETD system.

While the detection system has shown proficient ability to detect explosives at extremely low concentrations, the flow rate to the sensor may be too small to effectively interrogate large vapor headspaces in an acceptable amount of time. For example, CT tunnels have many liters of headspace that need to be interrogated in under a minute, in order to keep security lines moving at an appropriate speed. Flow

rates on the order of sccm would take far too long to interrogate this headspace and thus a method for higher volumetric sampling should be investigated. Heating the low thermal mass microheater in high flow rates may become a problem for this high volumetric sampling due to a cooling effect from the high velocity flows. Due to this cooling effect, a method for sampling low flow rates off of a bulk high flow rate should be investigated.

While the detection system works effectively by pulling ambient air into the system to be pushed towards the sensor devices by an air sampling pump, faster and more efficient methods could be achieved by reversing the air sampling pump such that analyte passes over the sensing elements before traveling throughout the remainder of the detection system. Currently, vapor must pass through devices such as MFCs and the air sampling pump before it reaches the sensor elements. If the flow through the ETD system was reversed, vapor would travel past the sensor elements first, thus reducing response time and possibly increasing sensitivity. In order for this reverse flow to be achieved, the entire detection system must be completely air tight such that suction can occur throughout the entire system.

BIBLIOGRAPHY

- [1] N. Gomes, “Trace Detection of TATP Vapors Using a Low-Mass Thermodynamic Sensor”, MS Thesis (2017) University of Rhode Island.
- [2] Z. Caron, “Novel Catalyst Development for Chemical Sensors”, MS Thesis (2016) The University of Rhode Island.
- [3] D. Mallin, “Increasing the Sensitivity and Selectivity of Gas Sensors for the Detection of Explosives”, MS Thesis (2014) The University of Rhode Island.
- [4] D. S. Moore, “Instrumentation for trace detection of high explosives”, *Review of Scientific Instruments*, 2004, vol. 75, pp. 2499.
- [5] “Explosion”, *Merriam Webster*. Accessed September 2018 from <https://www.merriam-webster.com/dictionary/explosion>.
- [6] J. Oxley, J. Smith, P. Bowden, and R. Rettinger, “Factors Influencing Triacetone Triperoxide (TATP) and Diacetone Diperoxide (DADP) Formation: Part I”, *Propellants, Explosives, and Pyrotechnics*. 2013, vol. 38, pp. 244 – 254.

- [7] R.S. Ladbeck, P. Kolla, U. Karst, "Trace analysis of peroxide-based explosives", *Anal. Chem.* 2013, vol. 75, pp. 731
- [8] H. Östmark, S. Wallin, H. Ghee Ang, "Vapor Pressure of Explosives: A Critical Review", *Propellants, Explosives, and Pyrotechnics*, February 2012, vol. 37 (1), pp 12-23.
- [9] X. Li, Z. Zhang, and L. Taoa, "A novel microarray chemiluminescence method based on chromium oxide nanoparticles catalysis for indirect determination of the explosive triacetone triperoxide at the scene", *Analyst*, 2013, vol. 138, pp. 1596-1600.
- [10] J. Oxley, J. Smith, H. Chen, "Decomposition of a Multi Peroxidic Compound: Triacetone Triperoxide (TATP)", *Propellants, Explosives, and Pyrotechnics*, September 2002, vol. 27 (4), pp. 209-216.
- [11] R. Hiyoshi, J. Nakamura, T. Brill, "Thermal Decomposition of Organic Peroxides TATP and HMTD by T-Jump/FTIR Spectroscopy", *Propellants, Explosives, and Pyrotechnics*, April 2007, vol. 32 (2), pp. 127-134.
- [12] "Four suicide bombers struck in central London on Thursday 7 July, killing 52 people and injuring more than 770", *BBC News*, accessed August 2018

from http://news.bbc.co.uk/2/shared/spl/hi/uk/05/london_blasts/what_happened/html/.

[13] “Brussels explosions: What we know about airport and metro attacks”, BBC News, accessed September 2018 from <https://www.bbc.com/news/world-europe-35869985>.

[14] “Manchester attack: Salman Abedi ‘made bomb in four days’ after potentially undergoing terror training in Libya”, *Independent*, October 2018 from <https://www.independent.co.uk/news/uk/home-news/manchester-attack-bombing-salman-abedi-isis-libya-terror-training-militants-tatp-four-days-bomb-a7771391.html>.

[15] “‘Mother of Satan’ explosives used in Surabaya church bombings: Police”, Asia One, accessed October 2018 from <http://www.asiaone.com/asia/mother-satan-explosives-used-surabaya-church-bombings-police>.

[16] S. Caygill, F. Davis, S. Higson, “Current trends in explosive detection techniques”, *Talanta*, Jan 2012, vol. 88, pp. 14-29.

[17] “Airport Security”, *Integrated Defense and Security Issues*, accessed September 2018 from <https://www.idsscorp.net/detect1000/>.

- [18] “TSA fails most tests at latest undercover operation at US airports”, *abc news*, accessed October 2018 from <https://abcnews.go.com/US/tsa-fails-tests-latest-undercover-operation-us-airports/story?id=51022188>.
- [19] G. Buttigieg, A. Knight, S. Denson, C. Pommier, M. Bonner Denton, “Characterization of the explosive triacetone triperoxide and detection by ion mobility spectrometry”, *Forensic Science International*, July 2003, vol. 135, pp53-59.
- [20] C. Mullen, A. Irwin, B.V. Pond, D.L. Huestis, M.J. Coggiola, H. Oser, “Detection of explosives and explosives-related compounds by single photon laser ionization time-of-flight mass spectrometry”, *Analytical Chemistry*, 2006, vol. 78, pp. 3807.
- [21] M. Sigman, C. Clark, R. Fidler, C. Geiger, C. Clausen, “Analysis of triacetone triperoxide by gas chromatography/mass spectrometry and gas chromatography/tandem mass spectrometry by electron and chemical ionization”, *Rapid Communications in Mass Spectrometry*, 2006, vol. 20, pp. 2851-2857.
- [22] R. Schulte-Ladbeck, Proceedings of the Pittsburgh Conference on Novel Analytical Methods for the Determination of Peroxide-Based Explosives (lecture 1336), Pittsburgh, 2002.

- [23] S. Hagenhoff, J. Franzke, H. Hayen, "Determination of Peroxide Explosive TATP and Related Compounds by Dielectric Barrier Discharge Ionization-Mass Spectrometry (DBDI-MS)", *Analytical Chemistry*, 2017, vol. 89 (7), pp 4210–4215.
- [24] E. Keinan, H. Itzhaky, "Method and kit for peroxidase detection of peroxide-type concealed explosives", Patent WO 9943846 (1999).
- [25] H. Lin, K. Suslick, "A Colorimetric Sensor Array for Detection of Triacetone Triperoxide Vapor", *American Chemical Society*, Oct 2010, vol. 132 (44), pp 15519–15521.
- [26] K. Brudzewskia, S. Osowskiab, W. Pawlowskia, "Metal oxide sensor arrays for detection of explosives at sub-parts-per million concentration levels by the differential electronic nose" *Sensors and actuators B: Chemical*, Jan 2012, vol 161 (1), pp 528-533.
- [27] "Keepers of the Gate", *Chemical and Engineering News*, accessed on October 2018 from <https://pubs.acs.org/cen/coverstory/87/8722cover.html>.

[28] K. Wells, D.A. Bradley, “A Review of X-ray Explosives Detection Techniques for Checked Baggage”, *University of Surrey*, accessed on October 2018 from <https://core.ac.uk/download/pdf/17180209.pdf>.

[29] “Budget Overview”, *Department of Homeland Security*, accessed September 2018 from <https://www.dhs.gov/sites/default/files/publications/S%26T%20FY18%20Budget.pdf>.

[30] “Oxidation States of Transition Metals”, *Chemistry LibreTexts*, accessed August 2018 from [https://chem.libretexts.org/Textbook_Maps/Inorganic_Chemistry/Supplemental_Modules_\(Inorganic_Chemistry\)/Descriptive_Chemistry/Elements_Organized_by_Block/3_dBlock_Elements/1b_Properties_of_Transition_Metals/Electron_Configuration_of_Transition_Metals/Oxidation_States_of_Transition_Metals](https://chem.libretexts.org/Textbook_Maps/Inorganic_Chemistry/Supplemental_Modules_(Inorganic_Chemistry)/Descriptive_Chemistry/Elements_Organized_by_Block/3_dBlock_Elements/1b_Properties_of_Transition_Metals/Electron_Configuration_of_Transition_Metals/Oxidation_States_of_Transition_Metals).

[31] “Heat of Reaction”, *Chemistry LibreTexts*, accessed September 2018 from [https://chem.libretexts.org/Textbook_Maps/Physical_and_Theoretical_Chemistry_Textbook_Maps/Supplemental_Modules_\(Physical_and_Theoretical_Chemistry\)/Thermodynamics/Energies_and_Potentials/Enthalpy/Heat_of_Reaction](https://chem.libretexts.org/Textbook_Maps/Physical_and_Theoretical_Chemistry_Textbook_Maps/Supplemental_Modules_(Physical_and_Theoretical_Chemistry)/Thermodynamics/Energies_and_Potentials/Enthalpy/Heat_of_Reaction).

- [32] E. G. Lavut, B. Timofeyev, V. Yuldasheva, E. A. Lavut, G. Galchenko, “Enthalpies of formation of tin (IV) and tin (II) oxides from combustion calorimetry” *Journal of Chemical Thermodynamics*, 1981, vol. 13 (7), pp. 635-646.
- [33] “Copper oxide”, *National Institute of Standards and Technology*, accessed September 2018 from <https://webbook.nist.gov/cgi/cbook.cgi?ID=C1317380&Mask=2>.
- [34] “Zinc oxide”, *National Institute of Standards and Technology*, accessed September 2018 from <https://webbook.nist.gov/cgi/cbook.cgi?ID=C1314132&Mask=2>.
- [35] B. Kim, J. Lee, H. Yoon, S. Kim. “Reduction of SnO₂ with Hydrogen”, *Materials Transactions*, 2011, vol 52, pp. 1814-1817.
- [36] Y. Zhu, K. Mimura, M. Isshiki, “Oxidation Mechanism of Copper at 623-1073K”, *Materials Transactions*, 2002, vol 4, pp 2173-2176.
- [37] S. Lew, A. F. Sarofim, M. Flytzani. “The reduction of Zinc Titanate and Zinc Oxide Solids”, *Chemical Engineering Science*, 1991, vol 47, pp 1412-1431.